Elevated Plasma Ghrelin Level in Underweight Patients with Chronic Obstructive Pulmonary Disease

Takefumi Itoh, Noritoshi Nagaya, Masanori Yoshikawa, Atsuhiko Fukuoka, Hideaki Takenaka, Yoshito Shimizu, Yoshinori Haruta, Hideo Oya, Masakazu Yamagishi, Hiroshi Hosoda, Kenji Kangawa, and Hiroshi Kimura

Department of Internal Medicine, National Cardiovascular Center, and Departments of Biochemistry and of Regenerative Medicine and Tissue Engineering, National Cardiovascular Center Research Institute, Osaka; Second Department of Internal Medicine, Nara Medical University, Nara; and Department of Respiratory Medicine, Chugoku Rousai Hospital, Hiroshima, Japan

Ghrelin, a novel growth hormone–releasing peptide, has been shown to cause a positive energy balance by reducing fat use and stimulating food intake. This study investigated whether plasma ghrelin is associated with clinical parameters in patients with chronic obstructive pulmonary disease. Plasma ghrelin was measured in 50 patients and 13 control subjects, together with anabolic and catabolic factors. Patients were divided into two groups based on body mass index: underweight patients (n = 26) or normal weight patients (n = 24). Plasma ghrelin was significantly higher in underweight patients than in normal weight patients and healthy control subjects. Circulating tumor necrosis factor-α, interleukin-6, and norepinephrine were significantly higher in underweight patients than in normal weight patients. Plasma ghrelin correlated negatively with body mass index and correlated positively with catabolic factors such as tumor necrosis factor-α and norepinephrine. In addition, plasma ghrelin correlated positively with percent predicted residual volume and residual volume-to-total lung capacity ratio. In conclusion, plasma ghrelin was elevated in underweight patients with chronic obstructive pulmonary disease, and the level was associated with a cachectic state and abnormality of pulmonary function.

Keywords: cachexia; ghrelin; hormone; pulmonary disease, chronic obstructive

Patients with chronic obstructive pulmonary disease (COPD) often show a certain degree of cachexia. Cachexia is an independent risk factor for mortality in such patients (1–3). Studies have shown that changes in endocrine hormones such as orexin and leptin have close relationships with cachexia associated with COPD (4–6). Growth hormone (GH) and its mediator, insulin-like growth factor (IGF)-I, are anabolic hormones that are essential for skeletal growth and metabolic homeostasis (7, 8). GH treatment has been shown to increase muscle mass in patients with COPD (9), although it has adverse effects including edema and abnormal glucose tolerance. These findings suggest a role of the GH/IGF-I axis in cachexia associated with COPD.

Ghrelin, a novel endogenous GH-releasing peptide, was isolated from the stomach (10). Ghrelin stimulates the secretion of GH through a mechanism independent from that of hypothalamic GH-releasing hormone. Ghrelin has been shown to cause a positive energy balance by reducing fat utilization through GH-independent mechanisms (11). In addition, both intracerebroventricular and peripheral administration of ghrelin have been shown to elicit potent, long-lasting stimulation of food intake via activation of neuropeptide Y neurons in the hypothalamic arcuate nucleus in animals (12–14). The plasma ghrelin level has been reported to be elevated in cachectic states (15, 16). However, little information is available regarding the pathophysiology of ghrelin in COPD.

Thus, the purposes of this study were to investigate (1) whether the plasma ghrelin level is elevated in patients with COPD, and (2) whether the plasma ghrelin level is related to a cachectic state and pulmonary function in patients with COPD.

METHODS

Subjects

We studied 50 patients with COPD (46 men and 4 women; mean age, 71 years; range, 41 to 83 years). COPD was diagnosed according to Global Initiative for Chronic Obstructive Lung Disease criteria. All patients were clinically stable at the time of evaluation. This study included 13 control subjects who had normal pulmonary function. The age and sex of the control subjects were similar to those of the 50 patients. The Institutional Review Board of Nara Medical University (Nara, Japan) approved this study. All subjects provided informed consent.

Patients with COPD were divided into two groups based on body mass index (BMI): underweight patients (BMI < 20, n = 26), or normal weight patients (BMI ≥ 20, n = 24). There was no significant difference in age, sex, smoking history, disease severity, or medication use between underweight and normal weight patients with COPD (Table 1). The mean smoking history was significantly higher in patients with COPD than in control subjects.

Fat-free mass (lean body mass) was measured by bioelectrical impedance analysis to investigate the relationship between plasma ghrelin and body composition in a subsample of 16 patients (underweight patients, n = 8; normal weight patients, n = 8). Lean body mass was significantly lower in underweight patients than in normal weight patients (39.3 ± 1.4 versus 46.5 ± 2.1 kg, $p < 0.05$).

Pulmonary Function Testing

Lung volumes were measured by the helium gas dilution method, and forced expiratory flow rates were measured with a mass flow anemometer (FUDAC 70; Fukuda Denshi, Tokyo, Japan). Carbon monoxide transfer factor was measured by the single-breath method. Pulmonary function values were expressed as a percentage of predicted values (17). Arterial blood gases were measured at rest with a blood gas analyzer (ABL 720; Radiometer, Brønshøj, Denmark).

Blood Sampling and Analysis

Blood samples were taken from the antecubital vein in the morning between 7:00 and 8:00 A.M. after an overnight fast. The blood was centrifuged immediately at 4°C and stored at –80°C. Plasma ghrelin was measured by radioimmunoassay as described previously (18).

Serum IGF-I was measured by radioimmunoassay (Somatomedin CII Bayer; Bayer Medical, Tokyo, Japan). Serum tumor necrosis

(Received in original form October 14, 2003; accepted in final form July 20, 2004)

Supported by the Mochida Memorial Foundation for Medical and Pharmaceutical Research and by grants from the Japan Cardiovascular Research Foundation, the New Energy and Industrial Technology Development Organization (NEDO), the Organization for Pharmaceutical Safety and Research (OPSR) of Japan (Promotion of Fundamental Studies in Health Science), and the Research Committee, Intractable Respiratory Failure, Ministry of Health, Labor, and Welfare of Japan.

Correspondence and requests for reprints should be addressed to Noritoshi Nagaya, M.D., Department of Regenerative Medicine and Tissue Engineering, National Cardiovascular Center Research Institute, 5-7-1 Fujishirodai, Suita, Osaka 565-8565, Japan. E-mail: nagayann@hsp.ncvc.go.jp

Am J Respir Crit Care Med Vol 170. pp 879–882, 2004
Originally Published in Press as DOI: 10.1164/rccm.200310-1404OC on July 21, 2004
Internet address: www.atsjournals.org

TABLE 1. PATIENT CHARACTERISTICS

	Control (*n* = 13)	COPD	
		Normal Weight (*n* = 24)	Underweight (*n* = 26)
Age, yr	69 ± 2	71 ± 2	71 ± 2
Sex, male/female	11/2	23/1	23/3
Body mass index, kg/m²	24.2 ± 0.7	24.2 ± 0.6	18.0 ± 0.3*,†
Smoking history, pack-years	17.6 ± 5.8	69.4 ± 6.2*	53.9 ± 5.9*
Severity stage, n			
I	NA	6	2
II	NA	5	7
III	NA	9	11
IV	NA	4	6
Medication use, n			
Anticholinergics	NA	11	16
β-Agonists	NA	15	14
Inhaled corticosteroids	NA	8	7
Xanthines	NA	14	14
Pulmonary function			
FEV_1, % predicted	93.0 ± 3.9	47.7 ± 4.4*	47.6 ± 3.5*
FEV_1/FVC, %	84.0 ± 2.3	41.4 ± 2.5*	41.7 ± 2.8*
VC, % predicted	95.7 ± 2.0	90.6 ± 5.5	84.8 ± 3.4
RV, % predicted		132.3 ± 7.8	152.0 ± 9.2
TLC, % predicted		101.2 ± 2.9	105.6 ± 3.9
RV/TLC, %		48.7 ± 2.3	52.8 ± 1.7
D_{LCO}, % predicted		61.6 ± 7.8	41.9 ± 5.5†
Pa_{O_2}, mm Hg		72.1 ± 1.7	71.4 ± 2.0
Pa_{CO_2}, mm Hg		44.5 ± 1.4	44.1 ± 1.6

Definition of abbreviations: D_{LCO} = diffusing capacity of the lung for carbon monoxide; NA = not applicable; RV = residual volume; RV/TLC, RV-to-TLC ratio; TLC = total lung capacity; VC = vital capacity.

Data represent means ± SEM.

*$p < 0.05$ versus control.

†$p < 0.05$ versus normal weight.

factor-α, interleukin-6, and insulin were measured by enzyme immunoassay (Quantikine HS [R&D Systems, Minneapolis, MN]; TFB kit [TFB, Tokyo, Japan]; and AIA-PACK IRI [Tosoh, Tokyo, Japan], respectively). Plasma epinephrine and norepinephrine were measured by high-performance liquid chromatography (HLC8030; Tosoh). Serum testosterone in male subjects was measured by radioimmunoassay (DPC testosterone kit; DPC, Los Angeles, CA). Serum prealbumin, retinol-binding protein, and transferrin were measured by nephelometry (Dade Behring, Deerfield, IL).

Statistical Analysis

Data are expressed as means ± SEM. Comparisons of parameters between the two groups were made by Fishes exact test or unpaired Student *t* test. Comparisons of parameters among three groups were made by one-way analysis of variance followed by the Scheffé multiple comparison test. Five groups (control subjects and patients with Stage I, II, III, and IV COPD) were compared by one-way analysis of variance followed by the Scheffé multiple comparison test. Independent relations between plasma ghrelin and pulmonary function parameters were examined by multivariate regression analyses. A p value less than 0.05 was considered statistically significant.

RESULTS

Biochemical Factors

Serum total protein and total cholesterol were significantly lower in underweight patients with COPD than in control subjects (Table 2). In addition, serum triglyceride, prealbumin, retinol-binding protein, and transferrin were significantly lower in underweight patients than in normal weight patients and control subjects.

TABLE 2. CIRCULATING LEVELS OF HORMONAL AND BIOCHEMICAL FACTORS

	Control (*n* = 13)	COPD	
		Normal Weight (*n* = 24)	Underweight (*n* = 26)
Total protein, g/dl	7.5 ± 0.1	7.2 ± 0.1	7.0 ± 0.1*
Albumin, g/dl	4.6 ± 0.1	4.5 ± 0.1	4.4 ± 0.1
Total cholesterol, mg/dl	221 ± 7	206 ± 6	192 ± 5*
Triglyceride, mg/dl	119 ± 9	106 ± 11	68 ± 4†,‡
Fasting glucose, mg/dl	109 ± 6	99 ± 4	97 ± 3
Prealbumin, mg/dl	30.3 ± 1.8	27.2 ± 0.8	23.0 ± 0.7†,‡
Retinol-binding protein, g/dl	4.6 ± 0.4	3.9 ± 0.2	3.0 ± 0.1†,‡
Transferrin, mg/dl	262 ± 7	228 ± 7*	202 ± 7†,§
Tumor necrosis factor-α, pg/ml	1.4 ± 0.1	4.3 ± 0.3†	6.8 ± 0.8†,‡
Interleukin-6, pg/ml	1.6 ± 0.3	2.3 ± 0.5	4.2 ± 0.7*,§
Epinephrine, pg/ml	43 ± 8	45 ± 6	59 ± 7
Norepinephrine, pg/ml	308 ± 19	674 ± 76*	982 ± 97†,§
Insulin-like growth factor-1, ng/ml	107 ± 6	137 ± 7*	114 ± 6§
Insulin, μU/ml	8.2 ± 0.8	7.0 ± 0.8	3.9 ± 0.6†,‡
Testosterone, ng/dl	419 ± 32	421 ± 19	484 ± 24

Data represent means ± SEM.

*$p < 0.05$ versus control.

†$p < 0.01$ versus control.

‡$p < 0.01$ versus normal weight.

§$p < 0.05$ versus normal weight.

Plasma Ghrelin and Cachectic State in Patients with COPD

The plasma ghrelin level was significantly higher in patients with COPD than in control subjects (237 ± 13 versus 157 ± 10 fmol/ml, $p < 0.01$). In particular, the plasma ghrelin level was higher in underweight patients than in normal weight patients and control subjects (272 ± 20 versus 195 ± 11 and 157 ± 10 fmol/ml, respectively, $p < 0.01$; Figure 1). The level did not significantly differ between normal weight patients and control subjects. The plasma ghrelin level correlated negatively with BMI ($r = -0.38$, $p < 0.01$; Figure 2). In addition, plasma ghrelin level correlated negatively with fat-free mass (lean body mass) ($r = -0.49$, $p < 0.05$) in a subsample of 16 patients.

Circulating levels of catabolic factors such as tumor necrosis factor-α and norepinephrine were significantly higher in both COPD groups than in control subjects (Table 2). Furthermore, the increases in these catabolic factors were marked in underweight patients compared with normal weight patients. On the other hand, circulating levels of anabolic factors such as IGF-1 and insulin were significantly lower in underweight patients than in normal weight patients, although these anabolic factors in normal weight patients ware increased (IGF-I) or unchanged (insulin) compared with those in control subjects. The plasma ghrelin level correlated positively with serum tumor necrosis

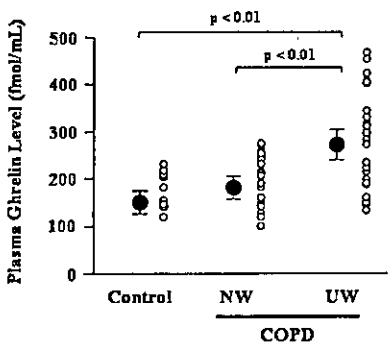

Figure 1. Plasma level of ghrelin in control subjects (Control), normal weight patients with chronic obstructive pulmonary disease (COPD) (NW), and underweight patients with COPD (UW).

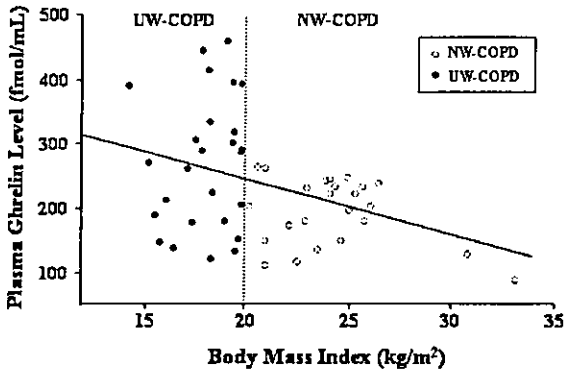

Figure 2. Correlation between plasma ghrelin level and body mass index in patients with COPD. Patients with COPD were divided into two groups: normal weight patients (NW-COPD) and underweight patients (UW-COPD). $r = -0.38$, $p < 0.01$.

factor-α ($r = 0.47$, $p < 0.01$) and plasma norepinephrine ($r = 0.40$, $p < 0.01$), but not serum IGF-I ($r = 0.12$, $p = 0.83$) and insulin ($r = -0.25$, $p = 0.27$). The plasma ghrelin level did not significantly differ between COPD patients with (n = 15) and without (n = 35) corticosteroid therapy (255 ± 27 versus 225 ± 14 fmol/ml, p = NS).

Plasma Ghrelin and Pulmonary Function in Patients with COPD

The plasma ghrelin level was higher in COPD patients with Stage IV disease than in control subjects (283 ± 31 versus 157 ± 10 fmol/ml, $p < 0.05$; Figure 3). Plasma ghrelin level tended to correlate negatively with percent predicted forced expiratory volume in one second ($r = -0.28$, $p = 0.07$), although the correlation did not reach statistical significance. Interestingly, plasma ghrelin level correlated positively with percent predicted residual volume ($r = 0.34$, $p < 0.05$) and residual volume-to-total lung capacity ratio ($r = 0.33$, $p < 0.05$) (Figure 4). Multiple regression analysis demonstrated that percent predicted residual volume or the residual volume-to-total lung capacity ratio was an independent determinant of plasma ghrelin level (each $p < 0.05$) even after adjustment for age, sex, and BMI. On the other hand, the plasma ghrelin level did not significantly correlate with any other pulmonary function parameters.

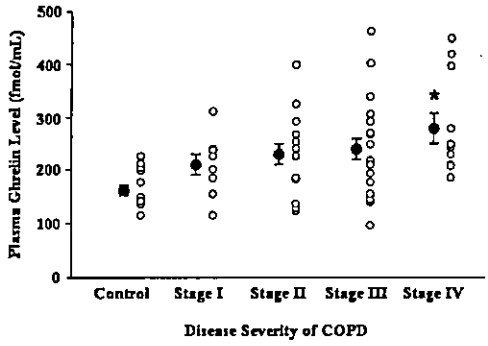

Figure 3. Plasma ghrelin level in patients with COPD according to disease severity based on Global Initiative for Chronic Obstructive Lung Disease guidelines. *$p < 0.05$ versus control.

DISCUSSION

In the present study, we demonstrated that (*1*) the plasma ghrelin level was elevated in underweight patients with COPD, and that (*2*) plasma ghrelin correlated negatively with BMI and correlated positively with circulating levels of tumor necrosis factor-α and norepinephrine. We also demonstrated that (*3*) the plasma ghrelin level was associated with indexes of hyperinflation including percent predicted residual volume and residual volume-to-total lung capacity ratio.

Ghrelin strongly stimulates GH release through a mechanism independent from that of hypothalamic GH-releasing hormone (10). Ghrelin has also been shown to cause a positive energy balance by reducing fat utilization and stimulating food intake (11–14). These findings suggest that ghrelin induces anabolic effects through GH-dependent and independent mechanisms. Thus, we investigated the pathophysiological significance of ghrelin in pulmonary cachexia. In the present study, we defined underweight as BMI < 20 kg/m². Some nutritional parameters including serum triglyceride, prealbumin, retinol-binding protein, and transferrin were also lower in underweight patients than in normal weight patients. These results suggest that "underweight" defined in the present study is accompanied by malnutrition. We demonstrated that plasma ghrelin level was higher in underweight patients than in normal weight patients. Furthermore, the plasma ghrelin level correlated negatively with BMI and lean body mass. These results suggest that the plasma ghrelin level is elevated in response to a cachectic state. Earlier studies have shown that hormonal changes and cytokine activation induce a catabolic state in patients with COPD, resulting in the development of cachexia (4–6, 19). In fact, some catabolic factors such as tumor necrosis factor-α, interleukin-6, and norepinephrine were significantly higher in underweight patients than in normal weight patients, whereas anabolic factors including IGF-I and insulin were significantly lower in underweight patients than in normal weight patients. The plasma ghrelin level correlated positively with catabolic factors such as tumor necrosis factor-α and norepinephrine. Considering the positive energy effects induced by ghrelin, increased ghrelin may represent a compensatory mechanism under catabolic–anabolic imbalance in cachectic patients with COPD. Unexpectedly, the serum IGF-I level was significantly higher in normal weight patients than in control subjects. Catabolic factors including tumor necrosis factor-α and norepinephrine were significantly higher in normal weight patients than in control subjects, although the increases were marked in underweight patients. These findings raise the possibility that increased IGF-I in normal weight patients may represent a compensatory mechanism under conditions of energy imbalance.

In the present study, the plasma ghrelin level showed significantly positive correlation with indexes of hyperinflation such as percent predicted residual volume and residual volume-to-total lung capacity ratio. In addition, the plasma ghrelin level tended to correlate negatively with percent predicted forced expiratory volume in 1 second. Thus, elevated ghrelin may be associated with abnormality of pulmonary function in patients with COPD. Because GH secretagogues receptor, a receptor for ghrelin, is expressed in the lung (20), further studies are to investigate a role of ghrelin in the lung. Although the present study demonstrated that body composition and indexes of hyperinflation were among the determinants of the plasma ghrelin level, further work will be required to determine the factors that contribute to the wide range of ghrelin levels among underweight patients with COPD.

In conclusion, the plasma ghrelin level was elevated in underweight patients with COPD, and the level was associated with a cachectic state and abnormality of pulmonary function.

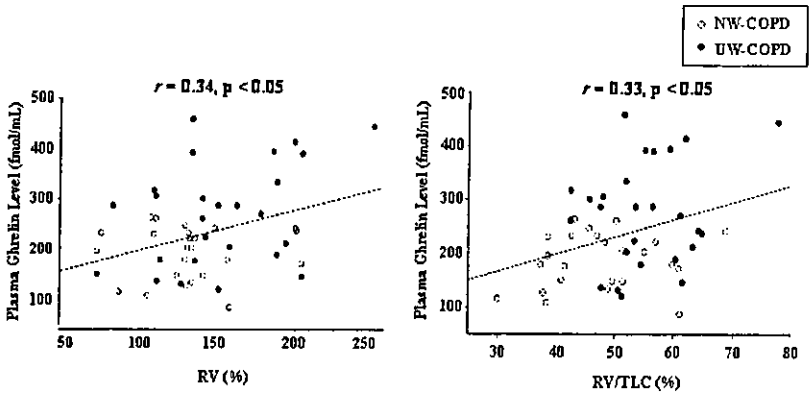

Figure 4. Correlations between plasma ghrelin level and percent predicted residual volume (RV, *left*), and between plasma ghrelin level and residual volume-to-total lung capacity ratio (RV/TLC, *right*) in patients with COPD. NW-COPD indicates normal weight patients with COPD; UW-COPD, underweight patients with COPD.

Conflict of Interest Statement: T.I. does not have a financial relationship with a commercial entity that has an interest in the subject of this manuscript; N.N. does not have a financial relationship with a commercial entity that has an interest in the subject of this manuscript; M.Y. does not have a financial relationship with a commercial entity that has an interest in the subject of this manuscript; A.F. does not have a financial relationship with a commercial entity that has an interest in the subject of this manuscript; H.T. does not have a financial relationship with a commercial entity that has an interest in the subject of this manuscript; Y.S. does not have a financial relationship with a commercial entity that has an interest in the subject of this manuscript; Y.H. does not have a financial relationship with a commercial entity that has an interest in the subject of this manuscript; H.O. does not have a financial relationship with a commercial entity that has an interest in the subject of this manuscript; M.Y. does not have a financial relationship with a commercial entity that has an interest in the subject of this manuscript; H.H. does not have a financial relationship with a commercial entity that has an interest in the subject of this manuscript; K.K. does not have a financial relationship with a commercial entity that has an interest in the subject of this manuscript; H.K. does not have a financial relationship with a commercial entity that has an interest in the subject of this manuscript.

References

1. Wilson DO, Rogers RM, Wright EC, Anthonisen NR. Body weight in chronic obstructive pulmonary disease: the National Institutes of Health Intermittent Positive Breathing Trial. *Am Rev Respir Dis* 1989; 139:1435–1438.
2. Gray-Donald K, Gibbons L, Shapiro SH, Macklem PT, Martin JG. Nutritional status and mortality in COPD. *Am J Respir Crit Care Med* 1996; 153:961–966.
3. Landbo C, Prescott E, Lange P, Vestbo J, Almdal TP. Prognostic value of nutritional status in chronic obstructive pulmonary disease. *Am J Respir Crit Care Med* 1999;160:1856–1861.
4. Takabatake N, Nakamura H, Minamihaba O, Inage M, Inoue S, Kagaya S, Yamaki M, Tomoike H. A novel pathophysiologic phenomenon in cachexic patients with chronic obstructive pulmonary disease: the relationship between the circadian rhythm of circulating leptin and the very low-frequency component of heart rate variability. *Am J Respir Crit Care Med* 2001;163:1314–1319.
5. Matsumura T, Nakayama M, Satoh H, Naito A, Kamahara K, Sekizawa K. Plasma orexin-A levels and body composition in COPD. *Chest* 2003; 123:1060–1065.
6. Debigare R, Marquis K, Cote CH, Tremblay RR, Michaud A, LeBlanc P, Maltais F. Catabolic/anabolic balance and muscle wasting in patients with COPD. *Chest* 2003;124:83–89.
7. Bark TH, McNurlan MA, Lang CH, Garlick PJ. Increased protein synthesis after acute IGF-I or insulin infusion is localized to muscle in mice. *Am J Physiol* 1998;275:E118–E123.
8. Amato G, Carella C, Fazio S, La Montagna G, Cittadini A, Sabatini D, Marciano-Mone C, Sacca L, Bellastella A. Body composition, bone metabolism, heart structure and function in growth hormone deficient adults before and after growth hormone replacement therapy at low doses. *J Clin Endocrinol Metab* 1993;77:1671–1676.
9. Burdet L, de Muralt B, Schutz Y, Pichard C, Fitting JW. Administration of growth hormone to underweight patients with chronic obstructive pulmonary disease: a prospective, randomized, controlled study. *Am J Respir Crit Care Med* 1997;156:1800–1806.
10. Kojima M, Hosoda H, Date Y, Nakazato M, Matsuo H, Kangawa K. Ghrelin is a growth-hormone releasing acylated peptide from stomach. *Nature* 1999;402:656–660.
11. Tschop M, Smiley DL, Heiman ML. Ghrelin induces adiposity in rodents. *Nature* 2000;407:908–913.
12. Wren AM, Small CJ, Ward HL, Murphy KG, Dakin CL, Taheri S, Kennedy AR, Roberts GH, Morgan DG, Ghatei MA, *et al.* The novel hypothalamic peptide ghrelin stimulates food intake and growth hormone secretion. *Endocrinology* 2000;141:4325–4328.
13. Nakazato M, Murakami N, Date Y, Kojima M, Matsuo H, Kangawa K, Matsukura S. A role for ghrelin in the central regulation of feeding. *Nature* 2001;409:194–198.
14. Shintani M, Ogawa Y, Ebihara K, Aizawa-Abe M, Miyanaga F, Takaya K, Hayashi T, Inoue G, Hosoda K, Kojima M, *et al.* Ghrelin, an endogenous growth hormone secretagogue, is a novel orexigenic peptide that antagonizes leptin action through the activation of hypothalamic neuropeptide Y/Y1 receptor pathway. *Diabetes* 2001;50:227–232.
15. Nagaya N, Uematsu M, Kojima M, Date Y, Nakazato M, Okumura H, Hosoda H, Shimizu W, Yamagishi M, Oya H, *et al.* Elevated circulating level of ghrelin in cachexia associated with chronic heart failure: relationships between ghrelin and anabolic/catabolic factors. *Circulation* 2001;23:2034–2038.
16. Shimizu Y, Nagaya N, Isobe T, Imazu M, Okumura H, Hosoda H, Kojima M, Kangawa K, Kohno N. Increased plasma ghrelin level in lung cancer cachexia. *Clin Cancer Res* 2003;9:774–778.
17. Berglund E, Birath G, Bjure J, Grimby G, Kjellmer I, Sandqvist L, Soderholm B. Spirometric studies in normal subjects. *Acta Med Scand* 1963;173:185–191.
18. Hosoda H, Kojima M, Matsuo H, Kangawa K. Ghrelin and des-acyl ghrelin: two major forms of rat ghrelin peptide in gastrointestinal tissue. *Biochem Biophys Res Commun* 2000;279:909–913.
19. Eid AA, Ionescu AA, Nixon LS, Lewis-Jenkins V, Matthews SB, Griffiths TL, Shale DJ. Inflammatory response and body composition in chronic obstructive pulmonary disease. *Am J Respir Crit Care Med* 2001;164: 1414–1418.
20. Gnanapavan S, Kola B, Bustin SA, Morris DG, McGee P, Fairclough P, Bhattacharya S, Carpenter R, Grossman AB, Korbonits M. The tissue distribution of the mRNA of ghrelin and subtypes of its receptor, GHS-R, in humans. *J Clin Endocrinol Metab* 2002;87:2988–2991.

Am J Physiol Heart Circ Physiol 287: H2670–H2676, 2004.
First published July 29, 2004; doi:10.1152/ajpheart.01071.2003.

Intravenous administration of mesenchymal stem cells improves cardiac function in rats with acute myocardial infarction through angiogenesis and myogenesis

Noritoshi Nagaya,[1,2] Takafumi Fujii,[3] Takashi Iwase,[1] Hajime Ohgushi,[4] Takefumi Itoh,[1] Masaaki Uematsu,[5] Masakazu Yamagishi,[2] Hidezo Mori,[3] Kenji Kangawa,[6] and Soichiro Kitamura[7]

Departments of [1]Regenerative Medicine and Tissue Engineering, [3]Cardiac Physiology, and [6]Biochemistry, National Cardiovascular Center Research Institute, Osaka 565-8565; Departments of [2]Internal Medicine and [7]Cardiovascular Surgery, National Cardiovascular Center, Osaka; [4]Tissue Engineering Research Center, National Institute of Advanced Industrial Science and Technology, Hyogo; and [5]Cardiovascular Division, Kansai Rosai Hospital, Hyogo 660-8511, Japan

Submitted 10 November 2003; accepted in final form 13 July 2004

Nagaya, Noritoshi, Takafumi Fujii, Takashi Iwase, Hajime Ohgushi, Takefumi Itoh, Masaaki Uematsu, Masakazu Yamagishi, Hidezo Mori, Kenji Kangawa, and Soichiro Kitamura. Intravenous administration of mesenchymal stem cells improves cardiac function in rats with acute myocardial infarction through angiogenesis and myogenesis. *Am J Physiol Heart Circ Physiol* 287: H2670–H2676, 2004. First published July 29, 2004; doi:10.1152/ajpheart.01071.2003.—Mesenchymal stem cells (MSCs) are pluripotent cells that differentiate into a variety of cells, including cardiomyocytes and endothelial cells. However, little information is available regarding the therapeutic potency of systemically delivered MSCs for myocardial infarction. Accordingly, we investigated whether intravenously transplanted MSCs induce angiogenesis and myogenesis and improve cardiac function in rats with acute myocardial infarction. MSCs were isolated from bone marrow aspirates of isogenic adult rats and expanded ex vivo. At 3 h after coronary ligation, 5×10^6 MSCs (MSC group, $n = 12$) or vehicle (control group, $n = 12$) was intravenously administered to Lewis rats. Transplanted MSCs were preferentially attracted to the infarcted, but not the noninfarcted, myocardium. The engrafted MSCs were positive for cardiac markers: desmin, cardiac troponin T, and connexin43. On the other hand, some of the transplanted MSCs were positive for von Willebrand factor and formed vascular structures. Capillary density was markedly increased after MSC transplantation. Cardiac infarct size was significantly smaller in the MSC than in the control group (24 ± 2 vs. $33 \pm 2\%$, $P < 0.05$). MSC transplantation decreased left ventricular end-diastolic pressure and increased left ventricular maximum dP/dt (both $P < 0.05$ vs. control). These results suggest that intravenous administration of MSCs improves cardiac function after acute myocardial infarction through enhancement of angiogenesis and myogenesis in the ischemic myocardium.

left ventricular end-diastolic pressure; cell transplantation; differentiation; homing

INTERRUPTION OF MYOCARDIAL blood flow leads to cardiomyocyte death (20). Although myocyte mitosis and the presence of cardiac precursor cells in adult hearts have recently been reported (6, 17), death of large numbers of cardiomyocytes results in the development of heart failure (16). Thus it would be desirable to induce angiogenesis and myogenesis for the treatment of ischemic heart disease.

Mesenchymal stem cells (MSCs) are pluripotent adult stem cells residing within the bone marrow microenvironment (11, 18). In contrast to their hematopoietic counterparts, MSCs have an adherent nature and are expandable in culture. MSCs can differentiate into not only osteoblasts, chondrocytes, neurons, and skeletal muscle cells but also vascular endothelial cells (19) and cardiomyocytes (23, 24). In vitro, MSCs have the potential to induce a neovascular response in murine Matrigel angiogenesis assay (2). In vivo, local MSC implantation induces therapeutic angiogenesis in a rat model of hindlimb ischemia (1). On the other hand, MSCs directly injected into the infarcted heart have been shown to induce myocardial regeneration and improve cardiac function (21). Stem or progenitor cells have been shown to circulate in peripheral blood and home to ischemic tissues (4). These results raise the possibility that intravenously administered MSCs participate in repair of the ischemic myocardium primarily by angiogenesis, which prevents apoptosis of native cardiomyocytes, and by direct regeneration of lost cardiomyocytes. However, little information is available regarding the therapeutic potential of systemically delivered MSCs for myocardial infarction.

Thus the purpose of this study was to investigate whether *1*) intravenously administered MSCs are able to engraft in the ischemic myocardium, *2*) transplanted MSCs induce angiogenesis and myogenesis after myocardial infarction, and *3*) transplantation of MSCs decreases infarct size and improves cardiac function.

METHODS

Animals. Male Lewis rats ($n = 70$) weighing 220–250 g were used in this study. These isogenic rats ($n = 8$) served as donors and recipients of MSCs to simulate autologous implantation. The Animal Care Committee of the National Cardiovascular Center approved the experimental protocol.

Model of myocardial infarction and cell transplantation. Fifty-one rats underwent ligation of the left coronary artery to produce myocardial infarction, as described previously (15). Briefly, after rats were anesthetized by injection of pentobarbital sodium (30 mg/kg body wt ip), they were artificially ventilated using a volume-regulated respirator. The heart was exposed via a left thoracotomy, and the left coronary artery was ligated 2–3 mm from its origin between the pulmonary artery conus and the left atrium using a 6-0 Prolene suture.

Address for reprint requests and other correspondence: N. Nagaya, Dept. of Regenerative Medicine and Tissue Engineering, National Cardiovascular Center Research Institute, 5-7-1 Fujishirodai, Suita, Osaka 565-8565, Japan (E-mail: nnagaya@ri.ncvc.go.jp).

The costs of publication of this article were defrayed in part by the payment of page charges. The article must therefore be hereby marked "*advertisement*" in accordance with 18 U.S.C. Section 1734 solely to indicate this fact.

At 3 h after coronary ligation, 40 rats survived (78% survival rate): 30 were randomized to receive an intravenous injection of MSCs (MSC group, $n = 14$) or PBS (control group, $n = 16$), and 10 received fluorescence-labeled MSCs for examination of MSC differentiation ($n = 5$) and incorporation ($n = 5$). Eleven rats underwent a sham operation consisting of thoracotomy and cardiac exposure but without coronary artery ligation. At 3 h after coronary ligation, we administered 5×10^6 MSCs/100 μl in PBS or PBS alone through a catheter inserted into the left jugular vein in ~30 s. The subsequent mortality for 4 wk was 25% in the control group and 14% in the MSC group. This protocol resulted in the creation of three groups: normal rats given PBS (sham group, $n = 11$), myocardial infarction rats given PBS (control group, $n = 12$), and myocardial infarction rats given MSCs (MSC group, $n = 12$).

Expansion of bone marrow MSCs. MSC expansion was performed according to previously described methods (18). Briefly, we killed the male Lewis rats and harvested the bone marrow by flushing the cavity of the femurs and tibias with PBS. Bone marrow cells were introduced into 100-mm dishes and cultured in α-MEM supplemented with 10% FBS and antibiotics. A small number of cells developed visible symmetrical colonies by *day 5–7*. Nonadherent hematopoietic cells were removed, and the medium was replaced. The adherent, spindle-shaped MSC population expanded to $>5 \times 10^7$ cells by approximately four to five passages after the cells were first cultured.

Flow cytometry. Adherent cells were analyzed by fluorescence-activated cell sorting (FACS SCAN flow cytometer, Becton Dickinson). Cells were incubated for 30 min at 4°C with the FITC-conjugated mouse monoclonal antibodies against rat CD34 (clone ICO-115, Santa Cruz Biotechnology) and CD45 and CD90 (clones OX-1 and OX-7, respectively, Becton Dickinson). FITC-conjugated hamster anti-rat CD29 monoclonal antibody (clone Ha2/5, Becton Dickinson) and rabbit anti-rat c-Kit polyclonal antibody (clone C-19, Santa Cruz Biotechnology) were used. Isotype-identical antibodies served as controls.

Echocardiographic studies. Echocardiographic studies were performed by an investigator blinded to treatment allocation 4 wk after coronary ligation. Two-dimensional targeted M-mode traces were obtained at the level of the papillary muscles using an echocardiographic system equipped with a 7.5-MHz phased-array transducer (SONOS 5500, Hewlett-Packard, Andover, MA). Anterior and posterior end-diastolic wall thickness and left ventricular (LV) end-diastolic and end-systolic dimensions were measured by the American Society for Echocardiology leading-edge method from at least three consecutive cardiac cycles. LV fractional shortening was calculated as follows: $(LVD_d - LVD_s)/LVD_d \times 100$, where LVD_d is LV diastolic dimension and LVD_s is LV systolic dimension. LV volume and ejection fraction were calculated on the basis of the Teichholtz formula.

Hemodynamic studies. Hemodynamic studies were performed 4 wk after coronary ligation. A 1.5-Fr micromanometer-tipped catheter (Millar Instruments) was inserted in the right carotid artery for measurement of mean arterial pressure. Then the catheter was advanced into the LV for measurement of LV pressure. Hemodynamic variables were measured using a pressure transducer (model P23 ID, Gould) connected to a polygraph. After completion of these measurements, the left and right ventricles were excised and weighed. Infarction size was determined as a percentage of the entire LV area, as reported previously (8). Briefly, incisions were made in the LV, so that the tissue could be pressed flat. The circumference of the entire flat LV and the visualized infarcted area, as judged from the epicardial and endocardial sides, was outlined on a clear plastic sheet. The difference in weight between the two marked areas on the sheet was used to determine infarction size and was expressed as a percentage of LV surface area.

Histological examination. To detect fibrosis in cardiac muscle, the LV myocardium ($n = 5$ each group) was fixed in 10% formalin, cut transversely, embedded in paraffin, and stained with Masson's trichrome. To detect capillary endothelial cells in the peri-infarct area, samples of the harvested muscle ($n = 5$ each) were embedded in OCT compound (Miles Scientific), snap frozen in liquid nitrogen, and cut into transverse sections. Tissue sections were stained for alkaline phosphatase with an indoxyltetrazolium method. The number of capillary vessels was counted in the peri-infarct area using a light microscope at ×200 magnification. The numbers in five high-power fields were averaged and expressed as the number of capillary vessels. These morphometric studies were performed by two examiners who were blinded to treatment.

An additional five rats were used to examine whether transplanted MSCs differentiated into cardiomyocytes or vascular endothelial cells. Suspended MSCs were labeled with fluorescent dyes with a PKH-26 red fluorescent cell linker kit (Sigma Chemical, St. Louis, MO) before implantation, as reported previously (13). Fluorescence-labeled MSCs were intravenously administered 3 h after coronary ligation. This subgroup of rats was killed 4 wk after coronary ligation. After the LV was excised and dissected free, muscle samples were embedded in OCT compound, snap frozen in liquid nitrogen, and cut into sections. Immunofluorescent staining for cardiac and endothelial cell markers was performed using monoclonal mouse antidesmin (Dako), anti-cardiac troponin T (Novo), anticonnexin43 (Sigma Chemical), and polyclonal rabbit anti-von Willebrand factor (Dako). FITC-conjugated IgG antibody (BD Pharmingen and Molecular Probes) was used as a secondary antibody.

At 24 h after intravenous administration of PKH-26-labeled MSCs, cardiac muscle was embedded in OCT compound and snap frozen in liquid nitrogen. Then the cardiac muscle from base to apex was

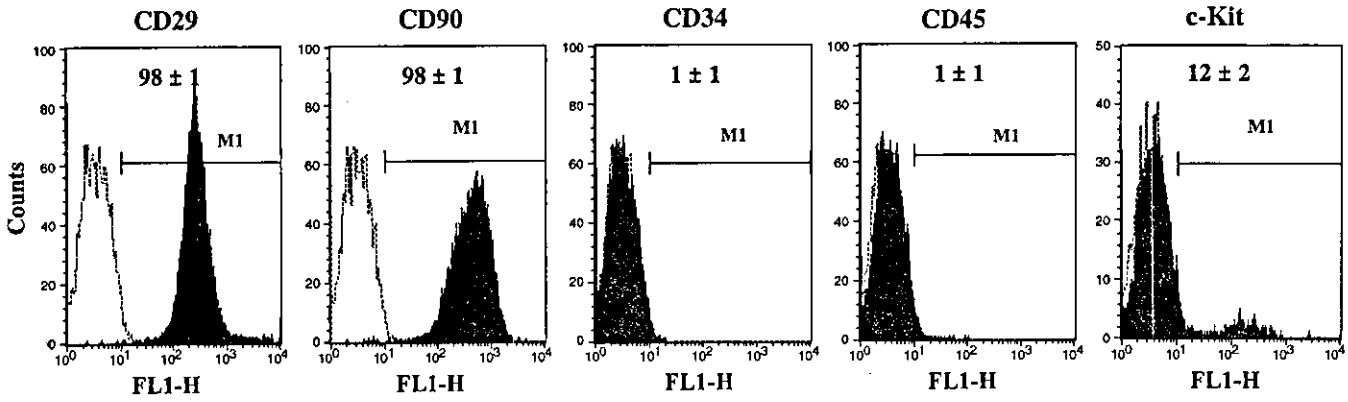

Fig. 1. Flow cytometric analysis of adherent, spindle-shaped mesenchymal stem cell (MSC) population expanded to 4–5 passages. Most of the cells expressed CD29 and CD90 but were negative for CD34 and CD45. Some cells were positive for c-Kit. MI, myocardial infarction.

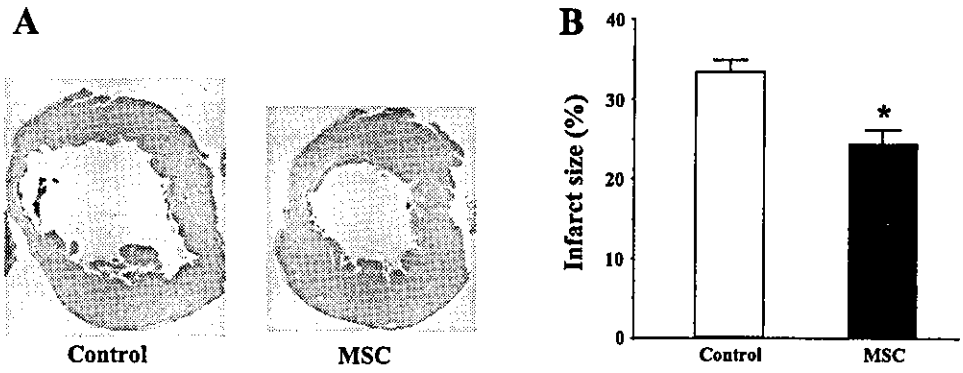

Fig. 2. Effect of MSC transplantation on myocardial infarct size 4 wk after myocardial infarction. *A*: representative Masson's trichrome-stained myocardial sections from control and MSC groups. *B*: quantitative analysis demonstrating that MSC transplantation significantly decreased infarct size. Values are means ± SE. $*P < 0.05$ vs. control.

transversely cut into 5-μm slices for calculation of the numbers of transplanted MSCs in the heart ($n = 5$).

Statistical analysis. Numerical values were expressed as means ± SE unless otherwise indicated. Comparisons of parameters among the three groups were made using one-way analysis of variance (ANOVA) followed by Scheffé's multiple comparison test. Comparisons of parameters between two groups were made by unpaired Student's *t*-test. $P < 0.05$ was considered significant.

RESULTS

Characterization of cultured MSCs. Most of cultured adherent cells expressed CD29 and CD90 (Fig. 1). In contrast, a majority of adherent cells were negative for CD34 and CD45. A small fraction of the adherent cells expressed c-Kit. Thus we confirmed that the major population of adherent cells was MSCs.

Reduction of myocardial infarct size after MSC transplantation. Moderate-to-large infarcts were observed in Masson's trichrome-stained myocardial sections 4 wk after coronary ligation (control group; Fig. 2*A*). However, MSC transplantation markedly decreased the infarct size after myocardial infarction (MSC group). Quantitative analysis also demonstrated that cardiac infarct size was significantly smaller in the MSC than in the control group: 24 ± 2 vs. 33 ± 2% ($n = 12$ each, $P < 0.05$; Fig. 2*B*).

Hemodynamic effects of MSC transplantation. At 4 wk after coronary ligation, hemodynamic studies were performed in the sham ($n = 11$), control ($n = 12$), and MSC ($n = 12$) groups. LV end-diastolic pressure showed a marked elevation in the control group (18 ± 1 mmHg); the elevation was significantly attenuated in the MSC group (13 ± 1 mmHg, $P < 0.05$; Fig. 3*A*). LV maximum dP/d*t* was significantly higher in the MSC than in the control group (Fig. 3*B*). LV minimum dP/d*t* tended to be lower in the MSC than in the control group (Fig. 3*C*). Although mean arterial pressure was significantly lower in the control than in the sham group, no decrease was observed in the MSC group (Table 1). Heart rate did not significantly differ among the three groups.

LV diastolic dimension was significantly smaller in the MSC than in the control group (Table 2). Fractional shortening was significantly greater in the MSC than in the control group (Fig. 3*D*). LV ejection fraction was also higher in the MSC than in

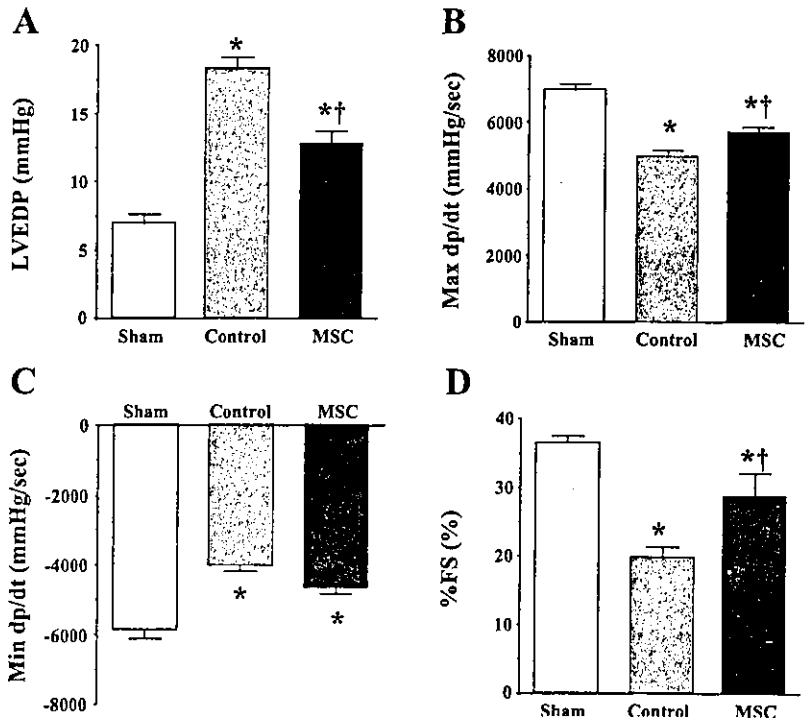

Fig. 3. Effects of MSC transplantation on hemodynamic parameters. LVEDP, LV end-diastolic pressure (*A*); max dP/d*t*, LV maximum dP/d*t* (*B*); Min dP/d*t*, LV minimum dP/d*t* (*C*); %FS, LV fractional shortening (*D*). Values are means ± SE. $*P < 0.05$ vs. sham. $\dagger P < 0.05$ vs. control.

Table 1. *Characterization of animals*

	Sham (n = 11)	Control (n = 12)	MSC (n = 12)
Body wt, g	331±4	301±7*	321±7†
LV wt/body wt, g/kg	1.83±0.11	2.22±0.10*	2.17±0.09*
RV wt/body wt, g/kg	0.55±0.02	0.83±0.04*	0.71±0.03*†
Heart rate, beats/min	404±15	428±17	418±15
Mean arterial pressure, mmHg	128±2	113±4*	119±3

Values are means ± SE. Sham, sham-operated rats given vehicle; control, myocardial infarction rats given vehicle; MSC, myocardial infarction rats given mesenchymal stem cells; LV, left ventricle; RV, right ventricle. *P < 0.05 vs. sham. †P < 0.05 vs. control.

Table 2. *Echocardiographic data*

	Sham	Control	MSC
LVD_d, mm	6.3±0.1	8.6±0.2*	7.5±0.3*†
LVD_s, mm	4.0±0.1	6.9±0.3*	5.5±0.5*†
%FS, %	37±1	20±2*	29±3*†
LVEF, %	65±1	39±3*	53±5*†
AWT diastole, mm	1.6±0.1	1.1±0.1*	1.4±0.1†
PWT diastole, mm	1.6±0.1	1.7±0.1	1.7±0.1

Values are means ± SE. LVD_d, LV diastolic dimension; LVD_s, LV systolic dimension; %FS, LV fractional shortening; LVEF, LV ejection fraction; AWT, anterior wall thickness; PWT, posterior wall thickness. *P < 0.05 vs. sham. †P < 0.05 vs. control.

the control group (Table 2). Diastolic anterior wall thickness was significantly attenuated in the MSC group compared with the control group.

Myogenesis and angiogenesis induced by MSCs. Red fluorescence-labeled MSCs were intravenously administered 3 h after coronary ligation (n = 5). Semiquantitative analysis demonstrated that ~3% of the transplanted MSCs were incorporated into the heart 24 h after transplantation. At 4 wk after transplantation (n = 5), MSCs were incorporated predominantly into the border zone of infarcts (Fig. 4), whereas few MSCs were detected in the noninfarcted myocardium. Immunofluorescence analyses demonstrated that the engrafted MSCs were positive for desmin (Fig. 4), cardiac troponin T (Fig. 5*A*), and connexin43 (Fig. 5*B*). These results suggest the ability of MSCs to engraft in the ischemic myocardium and differentiate into cardiomyocytes. On the other hand, some of the transplanted MSCs were positive for von Willebrand factor and formed vascular structures (Fig. 6). Alkaline phosphatase staining of the ischemic myocardium showed marked augmentation of neovascularization in the MSC group (Fig. 7*A*). Quantitative analysis demonstrated that capillary density was significantly higher in the MSC than in the control group (n = 5 each; Fig. 7*B*).

DISCUSSION

In the present study, we demonstrated that intravenously administered MSCs were capable of engraftment in the ischemic myocardium and that the engrafted MSCs differentiated into cardiomyocytes and vascular endothelial cells, resulting in myogenesis and angiogenesis. We also demonstrated that MSC transplantation decreased myocardial infarct size and improved cardiac function after acute myocardial infarction in rats.

Earlier studies showed that MSCs directly injected into the myocardium or those injected into coronary arteries improve cardiac function after myocardial infarction. However, little information is available regarding the therapeutic potential of systemically delivered MSCs for myocardial infarction. This study demonstrated that intravenous administration of MSCs

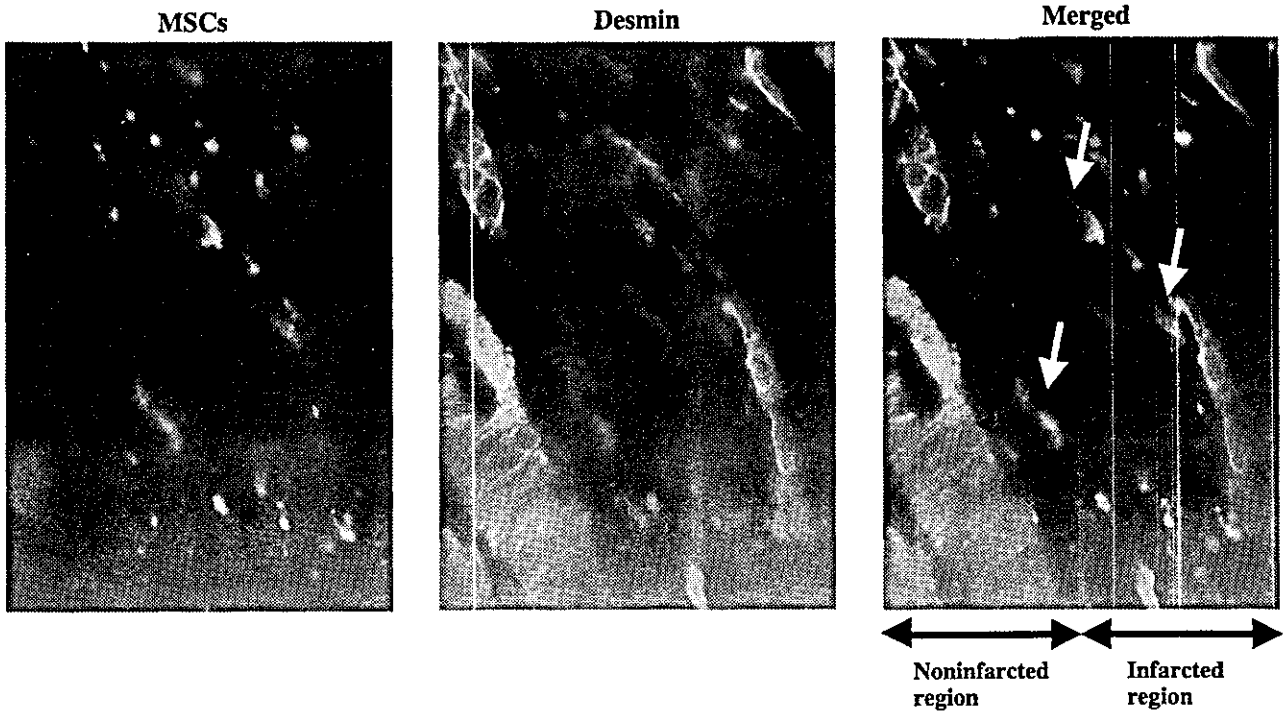

Fig. 4. Distribution of intravenously administered MSCs in myocardium after acute myocardial infarction. Red fluorescence-labeled MSCs were incorporated into ischemic boundary zone of the heart. These cells were positive for desmin (arrows), a cardiac marker. Magnification ×400.

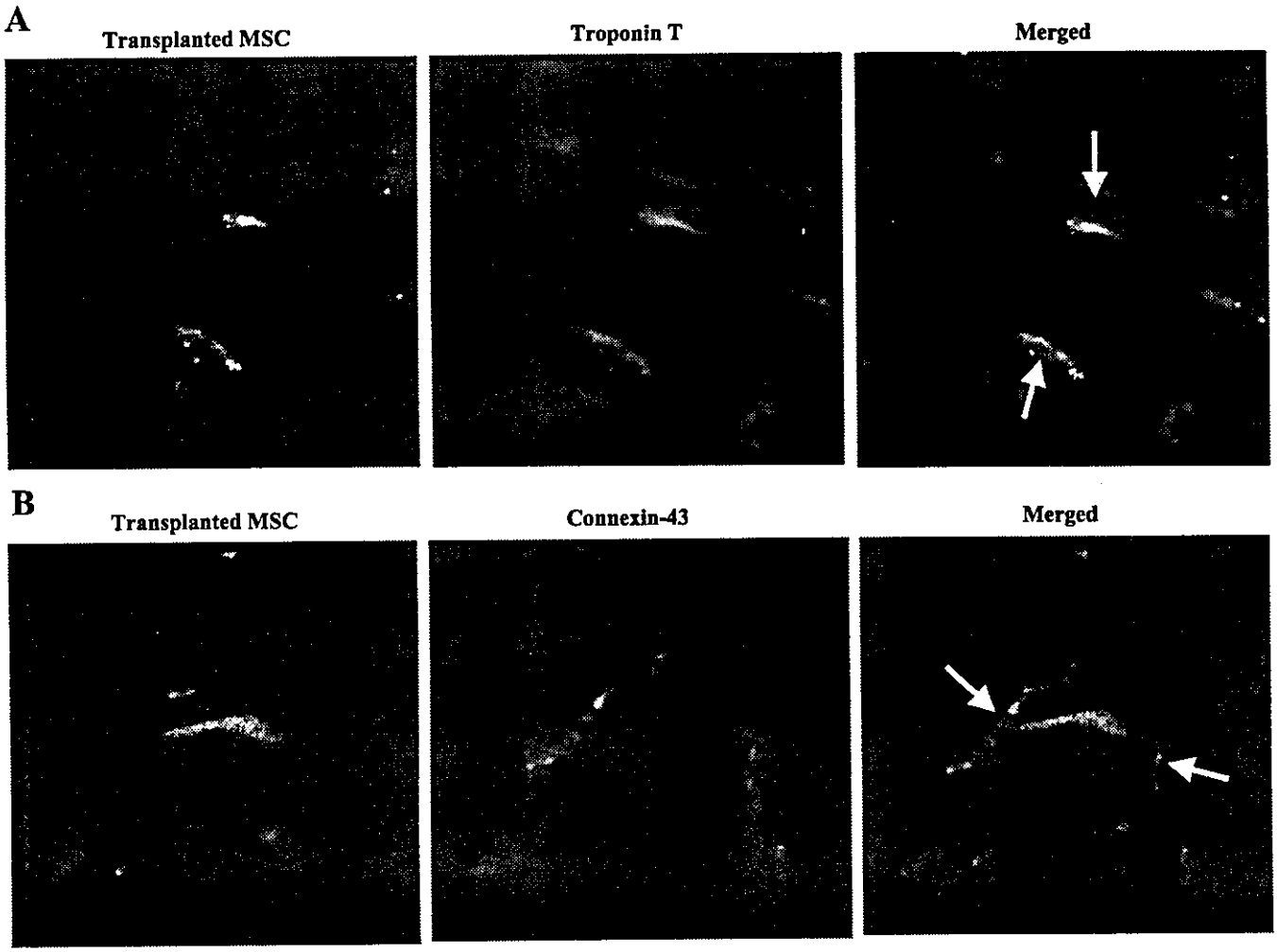

Fig. 5. Differentiation of transplanted MSCs in ischemic myocardium. Engrafted MSCs were positive (arrows) for cardiac troponin T (*A*) and connexin43 (*B*). Magnification ×400.

improves cardiac function after acute myocardial infarction through enhancement of angiogenesis and myogenesis in the ischemic myocardium.

Earlier studies showed that endothelial progenitor cells are mobilized from bone marrow into the peripheral blood in response to tissue ischemia and home to and incorporate into sites of neovascularization (21). Similar to epithelial progenitor cells, in the present study, transplanted MSCs were preferentially attracted to and retained in the border zone of infarcts. This is consistent with recent findings in the ischemic heart (5)

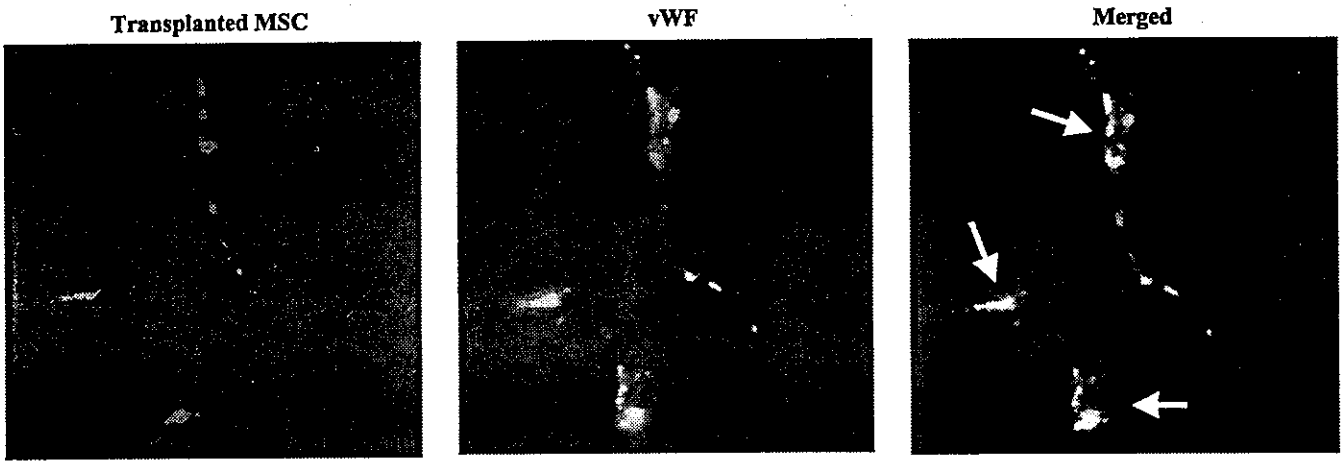

Fig. 6. Transplanted MSCs were positive for von Willebrand factor (vWF) and formed vascular structures. Magnification ×400.

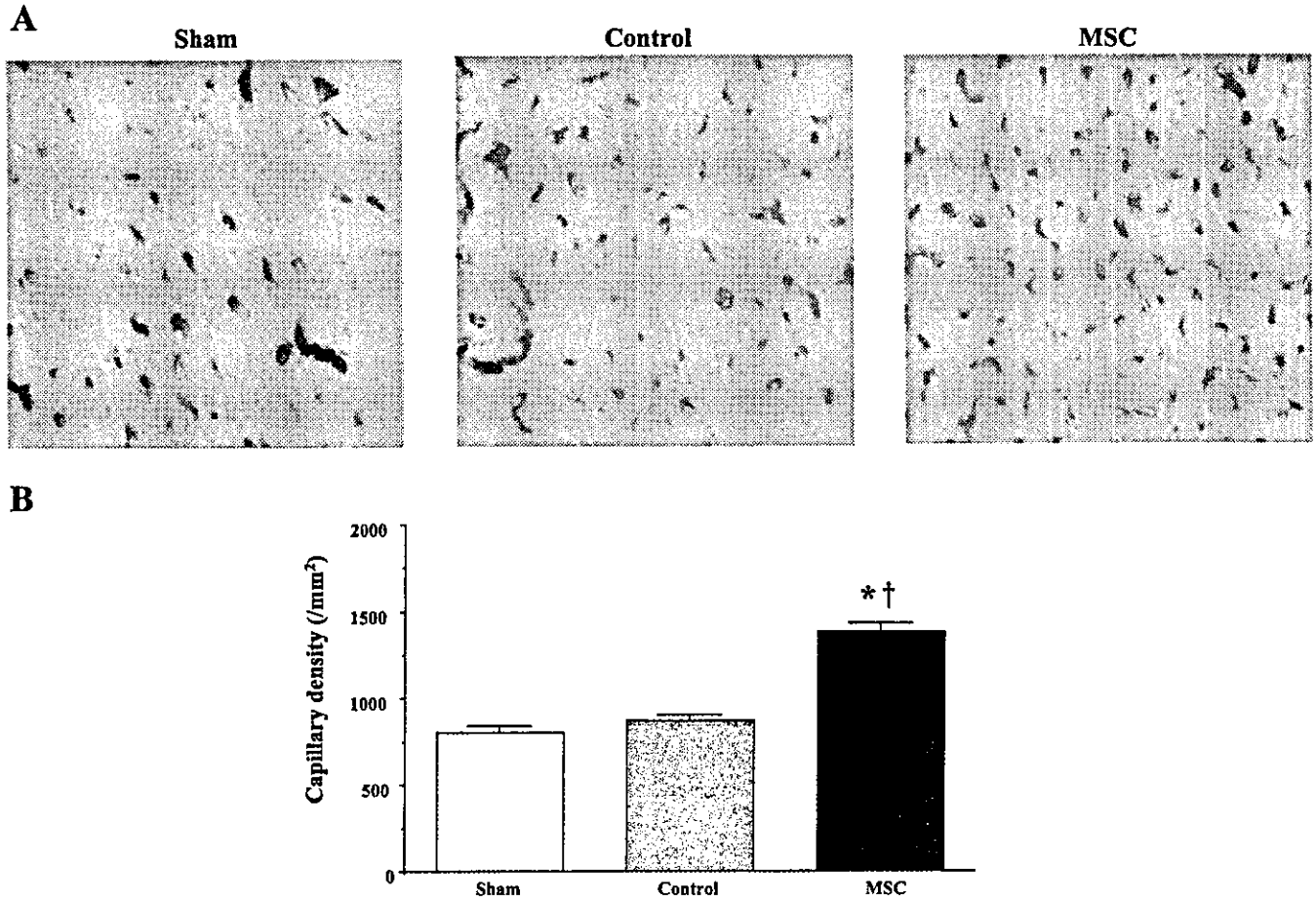

Fig. 7. *A*: representative samples of alkaline phosphatase staining in peri-infarct area. Magnification ×200. *B*: quantitative analysis of capillary density in peri-infarct area. Values are means ± SE. *$P < 0.05$ vs. sham. †$P < 0.05$ vs. control.

or brain (7). Although the underlying mechanisms remain unclear, ischemic tissue may express specific receptors or ligands to facilitate trafficking, adhesion, and infiltration of MSCs to ischemic sites.

In the present study, some of the engrafted MSCs were stained by cardiac proteins such as desmin and cardiac troponin T. Transplanted MSCs also expressed connexin43, a gap junction protein, at contact points with native cardiomyocytes. These results suggest that MSCs differentiated into cardiomyocytes in the ischemic myocardium and formed connections with native cardiomyocytes. In contrast to skeletal myoblasts, which have been used as a tool for myocardial repair, MSCs may have the capacity for electromechanical coupling. Earlier studies demonstrated the importance of the microenvironment for cardiomyogenic differentiation. Possible factors might include direct cell-cell contact (9), electrical and mechanical stimulation (10), and unknown growth factors. On the other hand, recent studies showed that stem cells may fuse with existing native cells (22, 25). Although the mechanisms by which MSCs develop into cardiomyocyte-like cells remain unclear, it is possible that the direct attachment with host cardiomyocytes in the ischemic myocardium contributes to the cardiogenic differentiation of transplanted MSCs. Further studies are necessary to investigate whether engrafted MSCs are actually becoming contractile.

In the present study, some of the transplanted MSCs were positive for an endothelial cell marker and participated in vessel formation. MSC transplantation significantly increased the capillary density in ischemic myocardium. The recently reported phenotypic plasticity of MSCs to transform into endothelial-like cells provides a rationale for their potential role in neovascularization. Hypoxia has been shown to induce MSC migration and capillary-like structure formation by upregulation of membrane type 1 matrix metalloproteinase (3). MSC implantation has been shown to induce therapeutic angiogenesis in a rat model of chronic hindlimb ischemia (1). These findings support the theory that intravenously administered MSCs are able to differentiate into vascular endothelial cells in the ischemic myocardium. Interestingly, MSCs enhance angiogenesis partly by increasing endogenous levels of vascular endothelial growth factor and vascular endothelial growth factor type 2 receptor (7). Together, these findings suggest that MSCs may contribute to neovascularization in the ischemic myocardium not only through their ability to generate capillary-like structures and but also through growth factor-mediated paracrine regulation.

The present study showed that MSC transplantation significantly reduced infarct size and attenuated wall thinning after acute myocardial infarction. Cardiomyocyte apoptosis during ischemia is one of the major contributors to the development of myocardial infarcts (16, 20). It is possible that newly formed vessels after MSC transplantation improve tissue perfusion around the ischemic boundary zone, resulting in functional recovery after acute myocardial infarction. We also demonstrated that transplanted

MSCs differentiated into cardiomyocytes in the ischemic myocardium. These results suggest that the decrease in infarct size and the increase in wall thickness may be attributable not only to MSC-induced neovascularization but also to myocardial regeneration. In the present study, MSC transplantation improved cardiac function after acute myocardial infarction, as indicated by a significant decrease in LV end-diastolic pressure, a tendency for an increase in maximum LV dP/d*t*, and a decrease in minimum LV dP/d*t*. Thus MSC-induced angiogenesis and myogenesis and the resultant reduced infarct size may have contributed to the hemodynamic improvement after acute myocardial infarction.

The low percentage of MSC migration to the heart is in agreement with some previous studies (5, 14). The present study also showed that only a small percentage of transplanted MSCs were incorporated into the heart. This may be explained by MSC apoptosis (12), tracking in the lung (5), and a dilution of the fluorescent dyes as the cells reproduce. Nevertheless, when MSCs were intravenously administered in an acute phase of myocardial infarction, MSCs induced angiogenesis and myogenesis and modestly, but significantly, improved cardiac function. Thus systemic delivery of MSCs may be beneficial for the treatment of myocardial infarction.

A limitation of this study is that the cell population may be mixed, rather than limited to MSCs, although cell surface markers of cultured cells were consistent with those of previously reported MSCs (12, 18).

In conclusion, intravenously administered MSCs were preferentially attracted to the infarcted myocardium and differentiated into vascular endothelial cells and cardiomyocytes. MSC transplantation decreased the infarct size and improved cardiac function after acute myocardial infarction through enhancement of angiogenesis and myogenesis. Thus MSC transplantation may be a new therapeutic strategy for the treatment of myocardial infarction.

GRANTS

This work was supported by Ministry of Health, Labour, and Welfare Cardiovascular Disease Research Grant 16C-6, the New Energy and Industrial Technology Development Organization of Japan Industrial Technology Research Grant Program in '03, Health and Labor Sciences Research Grants-genome 005, and Promotion of Fundamental Studies in Health Science of the Organization for Pharmaceutical Safety and Research of Japan.

REFERENCES

1. **Al-Khaldi A, Al-Sabti H, Galipeau J, and Lachapelle K.** Therapeutic angiogenesis using autologous bone marrow stromal cells: improved blood flow in a chronic limb ischemia model. *Ann Thorac Surg* 75: 204–209, 2003.
2. **Al-Khaldi A, Eliopoulos N, Martineau D, Lejeune L, Lachapelle K, and Galipeau J.** Postnatal bone marrow stromal cells elicit a potent VEGF-dependent neoangiogenic response in vivo. *Gene Ther* 10: 621–629, 2003.
3. **Annabi B, Lee YT, Turcotte S, Naud E, Desrosiers RR, Champagne M, Eliopoulos N, Galipeau J, and Beliveau R.** Hypoxia promotes murine bone-marrow-derived stromal cell migration and tube formation. *Stem Cells* 21: 337–347, 2003.
4. **Asahara T, Murohara T, Sullivan A, Silver M, van der Zee R, Li T, Witzenbichler B, Schatteman G, and Isner JM.** Isolation of putative progenitor endothelial cells for angiogenesis. *Science* 275: 964–967, 1997.
5. **Barbash IM, Chouraqui P, Baron J, Feinberg MS, Etzion S, Tessone A, Miller L, Guetta E, Zipori D, Kedes LH, Kloner RA, and Leor J.** Systemic delivery of bone marrow-derived mesenchymal stem cells to the infarcted myocardium: feasibility, cell migration, and body distribution. *Circulation* 108: 863–868, 2003.
6. **Beltrami AP, Urbanek K, Kajstura J, Yan SM, Finato N, Bussani R, Nadal-Ginard B, Silvestri F, Leri A, Beltrami CA, and Anversa P.** Evidence that human cardiac myocytes divide after myocardial infarction. *N Engl J Med* 344: 1750–1757, 2001.
7. **Chen J, Zhang ZG, Li Y, Wang L, Xu YX, Gautam SC, Lu M, Zhu Z, and Chopp M.** Intravenous administration of human bone marrow stromal cells induces angiogenesis in the ischemic boundary zone after stroke in rats. *Circ Res* 92: 692–699, 2003.
8. **Chien YW, Barbee RW, MacPhee AA, Frohlich ED, and Trippodo NC.** Increased ANF secretion after volume expansion is preserved in rats with heart failure. *Am J Physiol Regul Integr Comp Physiol* 254: R185–R191, 1988.
9. **Fukuhara S, Tomita S, Yamashiro S, Morisaki T, Yutani C, Kitamura S, and Nakatani T.** Direct cell-cell interaction of cardiomyocytes is key for bone marrow stromal cells to go into cardiac lineage in vitro. *J Thorac Cardiovasc Surg* 125: 1470–1480, 2003.
10. **Iijima Y, Nagai T, Mizukami M, Matsuura K, Ogura T, Wada H, Toko H, Akazawa H, Takano H, Nakaya H, and Komuro I.** Beating is necessary for transdifferentiation of skeletal muscle-derived cells into cardiomyocytes. *FASEB J* 17: 1361–1363, 2003.
11. **Makino S, Fukuda K, Miyoshi S, Konishi F, Kodama H, Pan J, Sano M, Takahashi T, Hori S, Abe H, Hata J, Umezawa A, and Ogawa S.** Cardiomyocytes can be generated from marrow stromal cells in vitro. *J Clin Invest* 103: 697–705, 1999.
12. **Mangi AA, Noiseux N, Kong D, He H, Rezvani M, Ingwall JS, and Dzau VJ.** Mesenchymal stem cells modified with Akt prevent remodeling and restore performance of infarcted hearts. *Nat Med* 9: 1195–1201, 2003.
13. **Messina LM, Podrazik RM, Whitehill TA, Ekhterae D, Brothers TE, Wilson JM, Burkel WE, and Stanley JC.** Adhesion and incorporation of lacZ-transduced endothelial cells into the intact capillary wall in the rat. *Proc Natl Acad Sci USA* 89: 12018–12022, 1992.
14. **Muller P, Pfeiffer P, Koglin J, Schafers HJ, Seeland U, Janzen I, Urbschat S, and Bohm M.** Cardiomyocytes of noncardiac origin in myocardial biopsies of human transplanted hearts. *Circulation* 106: 31–35, 2002.
15. **Nagaya N, Nishikimi T, Yoshihara F, Horio T, Morimoto A, and Kangawa K.** Cardiac adrenomedullin gene expression and peptide accumulation after acute myocardial infarction in rats. *Am J Physiol Regul Integr Comp Physiol* 278: R1019–R1026, 2000.
16. **Narula J, Haider N, Virmani R, DiSalvo TG, Kolodgie FD, Hajjar RJ, Schmidt U, Semigran MJ, Dec GW, and Khaw BA.** Apoptosis in myocytes in end-stage heart failure. *N Engl J Med* 335: 1182–1189, 1996.
17. **Oh H, Bradfute SB, Gallardo TD, Nakamura T, Gaussin V, Mishina Y, Pocius J, Michael LH, Behringer RR, Garry DJ, Entman ML, and Schneider MD.** Cardiac progenitor cells from adult myocardium: homing, differentiation, and fusion after infarction. *Proc Natl Acad Sci USA* 100: 12313–12318, 2003.
18. **Pittenger MF, Mackay AM, Beck SC, Jaiswal RK, Douglas R, Mosca JD, Moorman MA, Simonetti DW, Craig S, and Marshak DR.** Multilineage potential of adult human mesenchymal stem cells. *Science* 284: 143–147, 1999.
19. **Reyes M, Dudek A, Jahagirdar B, Koodie L, Marker PH, and Verfaillie CM.** Origin of endothelial progenitors in human postnatal bone marrow. *J Clin Invest* 109: 337–346, 2002.
20. **Saraste A, Pulkki K, Kallajoki M, Henriksen K, Parvinen M, and Voipio-Pulkki LM.** Apoptosis in human acute myocardial infarction. *Circulation* 95: 320–323, 1997.
21. **Shake JG, Gruber PJ, Baumgartner WA, Senechal G, Meyers J, Redmond JM, Pittenger MF, and Martin BJ.** Mesenchymal stem cell implantation in a swine myocardial infarct model: engraftment and functional effects. *Ann Thorac Surg* 73: 1919–1925, 2002.
22. **Terada N, Hamazaki T, Oka M, Hoki M, Mastalerz DM, Nakano Y, Meyer EM, Morel L, Petersen BE, and Scott EW.** Bone marrow cells adopt the phenotype of other cells by spontaneous cell fusion. *Nature* 416: 542–545, 2002.
23. **Toma C, Pittenger MF, Cahill KS, Byrne BJ, and Kessler PD.** Human mesenchymal stem cells differentiate to a cardiomyocyte phenotype in the adult murine heart. *Circulation* 105: 93–98, 2002.
24. **Wang JS, Shum-Tim D, Galipeau J, Chedrawy E, Eliopoulos N, and Chiu RC.** Marrow stromal cells for cellular cardiomyoplasty: feasibility and potential clinical advantages. *J Thorac Cardiovasc Surg* 120: 999–1005, 2000.
25. **Ying QL, Nichols J, Evans EP, and Smith AG.** Changing potency by spontaneous fusion. *Nature* 416: 545–548, 2002.

Am J Physiol Lung Cell Mol Physiol 287: L1172–L1177, 2004.
First published July 30, 2004; doi:10.1152/ajplung.00087.2004.

C-type natriuretic peptide attenuates bleomycin-induced pulmonary fibrosis in mice

Shinsuke Murakami,[1,2] Noritoshi Nagaya,[1,3] Takefumi Itoh,[2,3] Takafumi Fujii,[4] Takashi Iwase,[3] Kaoru Hamada,[2] Hiroshi Kimura,[2] and Kenji Kangawa[5]

[1]*Department of Internal Medicine, National Cardiovascular Center, Osaka 565-8565;* [2]*Second Department of Internal Medicine, Nara Medical University, Nara 634-8522;* [3]*Department of Regenerative Medicine and Tissue Engineering, National Cardiovascular Center Research Institute, Osaka 565-8565; and* [4]*Department of Cardiac Physiology and* [5]*Department of Biochemistry, National Cardiovascular Center Research Institute, Osaka 565-8565, Japan*

Submitted 12 March 2004; accepted in final form 21 July 2004

Murakami, Shinsuke, Noritoshi Nagaya, Takefumi Itoh, Takafumi Fujii, Takashi Iwase, Kaoru Hamada, Hiroshi Kimura, and Kenji Kangawa. C-type natriuretic peptide attenuates bleomycin-induced pulmonary fibrosis in mice. *Am J Physiol Lung Cell Mol Physiol* 287: L1172–L1177, 2004. First published July 30, 2004; doi:10.1152/ajplung.00087.2004.—C-type natriuretic peptide (CNP) has been shown to play an important role in the regulation of vascular tone and remodeling. However, the physiological role of CNP in the lung remains unknown. Accordingly, we investigated whether CNP infusion attenuates bleomycin (BLM)-induced pulmonary fibrosis in mice. After intratracheal injection of BLM or saline, mice were randomized to receive continuous infusion of CNP or vehicle for 14 days. CNP infusion significantly reduced the total number of cells and the numbers of macrophages, neutrophils, and lymphocytes in bronchoalveolar lavage fluid. Interestingly, CNP markedly reduced bronchoalveolar lavage fluid IL-1β levels. Immunohistochemical analysis demonstrated that CNP significantly inhibited infiltration of macrophages into the alveolar and interstitial regions. CNP infusion significantly attenuated BLM-induced pulmonary fibrosis, as indicated by significant decreases in Ashcroft score and lung hydroxyproline content. CNP markedly decreased the number of Ki-67-positive cells in fibrotic lesions of the lung, suggesting antiproliferative effects of CNP on pulmonary fibrosis. Kaplan-Meier survival curves demonstrated that BLM mice treated with CNP had a significantly higher survival rate than those given vehicle. These results suggest that continuous infusion of CNP attenuates BLM-induced pulmonary fibrosis and improves survival in BLM mice, at least in part by inhibition of pulmonary inflammation and cell proliferation.

inflammation; fibroblast; survival

PULMONARY FIBROSIS IS a life-threatening disease characterized by progressive dyspnea and worsening of pulmonary function (5). Most patients with pulmonary fibrosis are refractory to conventional therapy. The common pathological features observed in pulmonary fibrosis are infiltration of inflammatory cells, including activated macrophages and fibroblast proliferation with increased amounts of extracellular matrix (2). Thus a therapeutic strategy against these abnormalities may be effective for the treatment of pulmonary fibrosis.

C-type natriuretic peptide (CNP), the third member of the natriuretic peptide family consisting of 22 amino acid residues, is secreted by vascular endothelial cells (22, 24). CNP binds to natriuretic peptide receptor B, which bears a guanylate cyclase, induces generation of cGMP, and acts as a local regulator of vascular tone and remodeling (8, 23). Recently, CNP has been shown to suppress inflammation through inhibition of macrophage infiltration in injured carotid arteries of rabbits (20). Interestingly, CNP has been shown to directly inhibit cardiac fibroblast proliferation through a guanylate cyclase-B-mediated cGMP-dependent pathway (7). These findings suggest that CNP plays an important role in regulation of the cardiovascular system. However, the physiological role of CNP in the lung remains unknown. CNP mRNA and protein have been shown to be localized in bronchial airways and the alveolar epithelium (14). The respiratory epithelium has been shown to express a CNP-specific receptor (4). These findings raise the possibility that CNP may have protective effects against pulmonary inflammation and fibroblast proliferation, both of which are responsible for pulmonary fibrosis.

Thus the purposes of this study were *1*) to investigate whether continuous infusion of CNP attenuates bleomycin (BLM)-induced pulmonary fibrosis in mice, *2*) to investigate whether CNP infusion improves survival in BLM-treated mice, and *3*) to examine the underlying mechanisms responsible for the effects of CNP on pulmonary fibrosis.

METHODS

Animals. We used specific pathogen-free 10-wk-old female C57BL/6 mice weighing 18–20 g. The mice were randomly given an intratracheal injection of either BLM (Nippon Kayaku, Tokyo, Japan) or 0.9% saline and assigned to receive continuous infusion of CNP or vehicle. This protocol resulted in the creation of three groups: sham mice given vehicle (Sham group, $n = 27$), BLM mice given vehicle (vehicle group, $n = 55$), and BLM mice treated with CNP (CNP group, $n = 55$). All protocols were performed in accordance with guidelines of the Animal Care Ethics Committee of the National Cardiovascular Center Research Institute (Osaka, Japan).

Experimental protocol. After the mice were anesthetized by intraperitoneal injection of pentobarbital sodium, they were given an intratracheal injection of either BLM (0.02 or 0.04 U/mouse) dissolved in 50 μl of 0.9% sterile saline or saline alone. Then, an osmotic minipump (Alzet, Palo Alto, CA) was filled with either CNP to deliver a dose of 0.06 μg/h or 5% glucose vehicle throughout the experiment and implanted subcutaneously on the back, slightly caudal to the scapulae. The mice were maintained under standard conditions with free access to food and water.

Address for reprint requests and other correspondence: N. Nagaya, Dept. of Regenerative Medicine and Tissue Engineering, National Cardiovascular Center Research Institute, 5-7-1 Fujishirodai, Suita, Osaka 565-8565, Japan (E-mail: nnagaya@ri.ncvc.go.jp).

The costs of publication of this article were defrayed in part by the payment of page charges. The article must therefore be hereby marked "*advertisement*" in accordance with 18 U.S.C. Section 1734 solely to indicate this fact.

Table 1. *Physiological profiles of three experimental groups*

	Sham group	Vehicle group	CNP group
Low dose (0.02 U/mouse) of BLM			
n	7	8	9
Body weight, g	21.2±0.3	18.3±0.4*	20.2±0.3†
Lung weight/body weight, mg/g	6.1±0.1	12.9±0.5*	7.9±0.2*†
	Sham group	Vehicle group	CNP group
High dose (0.04 U/mouse) of BLM			
n	7	7	9
Body weight, g	21.2±0.3	15.7±1.1*	19.9±0.6†
Lung weight/body weight, mg/g	6.1±0.1	18.4±2.0*	12.5±1.1*†

Values are means ± SE. Measurements were performed 14 days after bleomycin (BLM) injection. Sham group, sham mice given vehicle; vehicle group, BLM mice given vehicle; CNP group, BLM mice treated with C-type natriuretic peptide. *$P < 0.05$ vs. Sham group; †$P < 0.05$ vs. vehicle group.

Mice treated with 0.02 units of BLM were used to assess the antifibrotic effects of CNP. Histological examination and measurement of lung hydroxyproline content were performed at 14 days. Cell proliferation detected by Ki-67 was also evaluated in mice given 0.02 units of BLM. Survival rate in mice given 0.02 units of BLM was relatively high (80%). On the other hand, mice treated with 0.04 units of BLM were used to assess the effects of CNP on pulmonary inflammation and survival. After anesthesia with pentobarbital sodium, bronchoalveolar lavage (BAL) was performed at 1, 3, 7, and 14 days. Macrophage infiltration was also evaluated 14 days after injection of 0.04 units of BLM. The wet lung weight was measured, and the wet lung weight-to-body weight ratio was then calculated at 14 days in mice not subjected to BAL.

Survival analysis. To evaluate the effect of CNP on survival in BLM mice, 60 mice received continuous infusion of CNP ($n = 30$) or vehicle ($n = 30$) for 14 days. Survival was estimated from the date of BLM injection to the death of the mouse or 14 days after injection.

BAL analysis. BAL was performed through a tracheal cannula with 1 ml of saline solution ($n = 5$ each). This procedure was repeated three times. A 500-μl aliquot of BAL fluid (BALF) was reserved for determination of the total number of cells and cell differentiation, and the remainder was centrifuged immediately at 800 *g* for 10 min at 4°C. We counted the total number of cells using a standard hemocytometer. We examined cell differentiation by counting at least 200 cells on a smear prepared using cytospin and Wright-Giemsa staining.

Enzyme-linked immunosorbent assay. The supernatant of BALF was immediately stored at −80°C until the assay. We measured BALF TNF-α and BALF IL-1β levels with a mouse TNF-α ELISA kit (Pierce Chemical, Rockford, IL) and mouse IL-1β ELISA kit (Biosource International, Camarillo, CA), respectively ($n = 5$ each).

Histological examination. The right lung was fixed with 4% paraformaldehyde and embedded in paraffin ($n = 5$ each). Sections 4-μm thick were stained with hematoxylin-eosin. The Ashcroft score was used for semi-quantitative assessment of fibrotic changes (1). The severity of fibrotic changes in each histological section of the lung was assessed as the mean score of severity from observed microscopic fields. Thirty fields in each section were analyzed. Grading was done in a blinded fashion by two observers, and the mean was taken as the fibrosis score.

Measurement of hydroxyproline content. To quantify lung collagen content as an indicator of pulmonary fibrosis, the hydroxyproline content in the lung was measured in each group according to the previously described method ($n = 5$ each) (15). The left lung was frozen and kept at −80°C until the assay. After the lung was homogenized, the suspension was hydrolyzed with 0.5 ml of 12 N hydrochloric acid for 20 h at 100°C. After neutralization, a 0.1-ml aliquot of supernatant was mixed in 1.5 ml of 0.3 N lithium hydroxide solution. The hydroxyproline content was analyzed by high-performance chromatography.

Immunohistochemistry. Paraffin sections 4-μm thick were obtained from the lung ($n = 5$ each). To investigate whether CNP inhibits macrophage infiltration, tissue sections were stained for F4/80, a

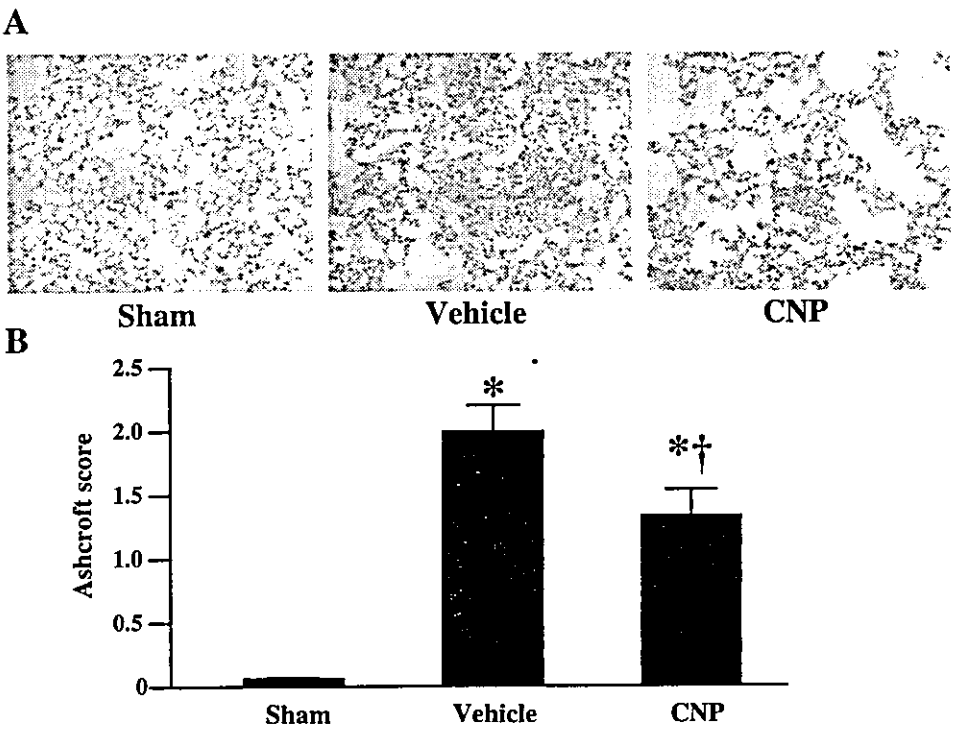

Fig. 1. *A*: representative photomicrographs of lung tissues stained with hematoxylin-eosin. Histological sections were taken from the same general regions of the lungs in each group. Intratracheal injection of bleomycin (BLM) induced pulmonary fibrosis in mice (vehicle group) compared with mice given vehicle (Sham group). C-type natriuretic peptide (CNP) infusion attenuated pulmonary fibrosis in BLM mice (CNP group). Magnification, ×100. *B*: semi-quantitative analyses of lung tissues using the Ashcroft score, a marker for pulmonary fibrosis. The score was significantly decreased in the CNP group. Data are means ± SE. *$P < 0.05$ vs. Sham group; †$P < 0.05$ vs. vehicle group.

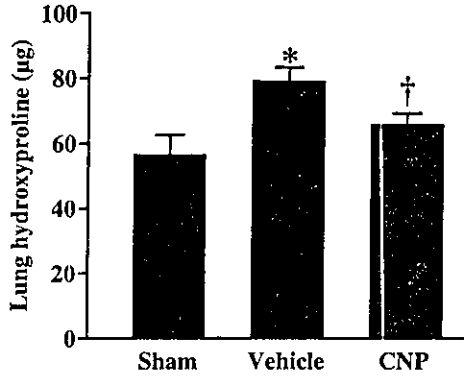

Fig. 2. Effects of CNP infusion on hydroxyproline content in left lung of BLM mice (n = 5 each). BLM injection increased lung hydroxyproline content (vehicle group). CNP infusion significantly decreased hydroxyproline content in BLM mice (CNP group). Data are means ± SE. *P < 0.05 vs. Sham group; †P < 0.05 vs. vehicle group.

murine monocyte/macrophage membrane antigen, using rat anti-mouse F4/80 IgG (Serotec, Oxford, UK). To investigate whether CNP inhibits cell proliferation of pulmonary fibrosis, we stained tissue sections for Ki-67, a marker for cell proliferation, using rat anti-mouse Ki-67 antibody (DAKO, Copenhagen, Denmark). The numbers of F4/80-positive cells and Ki-67-positive cells were determined in 10 randomly chosen fields (×400).

Statistical analysis. All data are expressed as means ± SE unless otherwise indicated. Comparisons of parameters among the three groups were made by one-way ANOVA, followed by Newman-Keuls test. Survival curves were derived by the Kaplan-Meier method and compared by log-rank test. A value of P < 0.05 was considered statistically significant.

RESULTS

Physiological profiles. The physiological profiles of the three experimental groups are shown in Table 1. Body weight was significantly lower in BLM mice given vehicle (vehicle group) than in normal mice given vehicle (Sham group) and in BLM mice treated with CNP (CNP group). However, there was no significant difference between the Sham and CNP groups. Wet lung weight-to-body weight ratio was significantly increased after BLM injection. However, the increase in the CNP group was significantly attenuated compared with that in the vehicle group.

Inhibition of pulmonary fibrosis by CNP. The normal alveolar structure was maintained in the Sham group (Fig. 1*A*). Fourteen days after BLM injection, the alveolar wall was thickened and the air spaces were collapsed in the vehicle group. In addition, focal fibrotic lesions were observed. In contrast to the findings in mice treated with BLM alone, fibrotic lesions were less focal in the CNP group. Semiquantitative assessment using Ashcroft score demonstrated that the degree of pulmonary fibrosis in the CNP group was lower than that in the vehicle group (Fig. 1*B*). The hydroxyproline content in the lung was significantly increased after BLM injection (Fig. 2). However, the content in the CNP group was significantly lower than that in the vehicle group.

Anti-inflammatory effects of CNP. The recovery rate of BALF was over 80% in all groups. The total number of cells and the number of macrophages were significantly increased at 3, 7, and 14 days after BLM injection (Fig. 3, *A* and *B*). However, the numbers of these cells in the CNP group were significantly lower than those in the vehicle group. The number of neutrophils was significantly increased at 1, 3, 7, and 14 days after BLM injection (Fig. 3*C*). However, the number of these in the CNP group was significantly lower than that in the vehicle group at 7 and 14 days after BLM injection. The number of lymphocytes was significantly increased at 3, 7, and 14 days after BLM injection (Fig. 3*D*). However, the number of these in the CNP group was significantly lower than that in the vehicle group at 3 and 7 days after BLM injection. The BALF IL-1β level was significantly increased at 3 and 14 days after BLM injection (Fig. 4*A*). However, CNP infusion markedly inhibited the increase in BALF IL-1β level. The BALF TNF-α level was significantly increased at 3 days after BLM injection (Fig. 4*B*). CNP infusion tended to inhibit the increase in BALF TNF-α level, but this was not significant (P = 0.058).

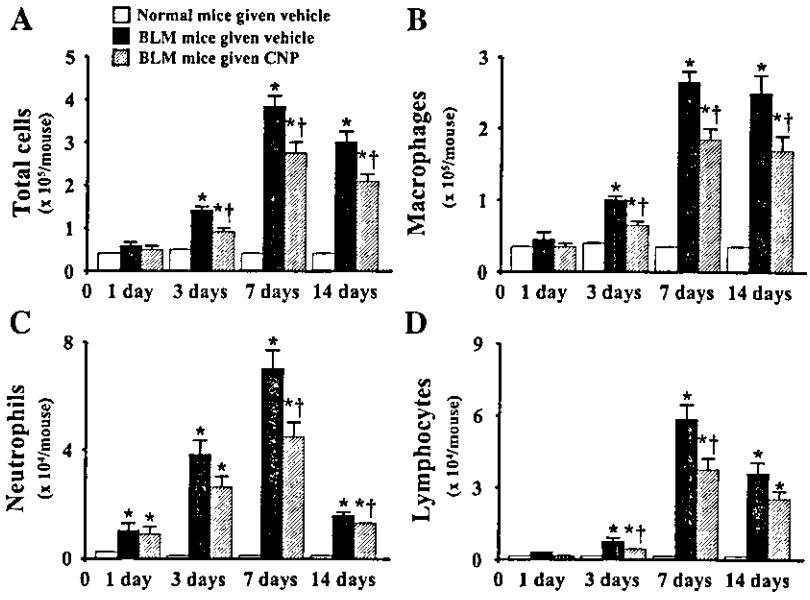

Fig. 3. Effects of CNP infusion on the numbers of total cells (*A*), macrophages (*B*), neutrophils (*C*), and lymphocytes (*D*) in bronchoalveolar lavage fluid (BALF). The total number of cells and the number of macrophages were significantly increased at 3, 7, and 14 days after BLM injection. However, the numbers of these cells in the CNP group were significantly lower than those in the vehicle group. The number of neutrophils was significantly increased at 1, 3, 7, and 14 days after BLM injection. However, the number of these in the CNP group was significantly lower than that in the vehicle group at 7 and 14 days after BLM injection. The number of lymphocytes was significantly increased at 3, 7, and 14 days after BLM injection. However, the number of these in the CNP group was significantly lower than that in the vehicle group at 3 and 7 days after BLM injection. Data are means ± SE. *P < 0.05 vs. Sham group, †P < 0.05 vs. vehicle group.

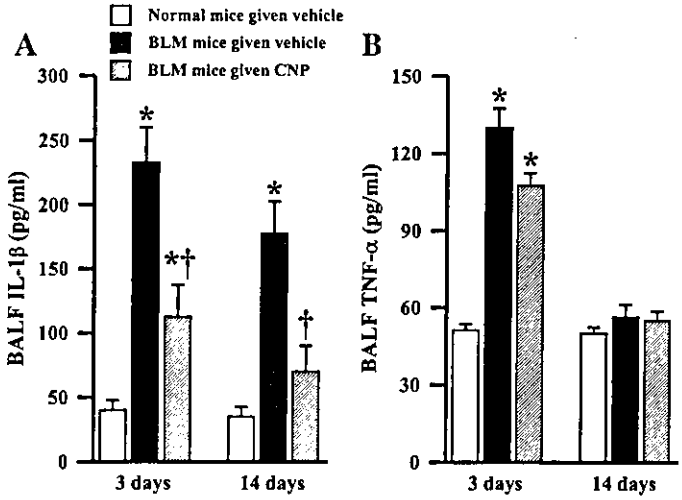

Fig. 4. Effects of CNP infusion on BALF IL-1β (*A*) and BALF TNF-α (*B*) levels at 3 and 14 days after BLM injection. CNP significantly decreased BALF IL-1β level. CNP tended to inhibit the increase in BALF TNF-α level, but this was not significant ($P = 0.058$). Data are means ± SE. *$P < 0.05$ vs. Sham group, †$P < 0.05$ vs. vehicle group.

Representative photomicrographs showed that CNP infusion markedly inhibited macrophage infiltration compared with vehicle (Fig. 5*A*). Semi-quantitative analysis demonstrated that BLM injection significantly increased the number of macrophages (Fig. 5*B*). However, the increase was markedly inhibited in the CNP group.

Antiproliferative effects of CNP. Unlike sham mice, Ki-67-positive cells were frequently observed mainly in fibrotic lesions 14 days after BLM injection (Fig. 6*A*). Interestingly, CNP infusion markedly decreased Ki-67-positive cells in the fibrotic lesions. Semi-quantitative analysis demonstrated that the number of Ki-67-positive cells was significantly decreased in the CNP group compared with that in the vehicle group (Fig. 6*B*).

Survival analysis. Kaplan-Meier survival curves demonstrated that BLM mice treated with CNP had a significantly higher survival rate than those given vehicle (70% vs. 40% 14-day survival, log-rank test, $P < 0.01$, Fig. 7).

DISCUSSION

In the present study, we demonstrated that *1*) continuous infusion of CNP attenuated BLM-induced pulmonary fibrosis, as indicated by decreases in Ashcroft score and lung hydroxyproline content, *2*) CNP inhibited cellular infiltration in the lung and decreased BALF IL-1β levels in BLM mice, and *3*) infusion of CNP decreased the number of Ki-67-positive cells in fibrotic lesions of the lung. Finally, we demonstrated that *4*) CNP infusion increased the survival rate in BLM mice.

BLM, an antineoplastic antibiotic, has been reported to induce pulmonary fibrosis dose dependently when intratracheally injected in experimental animals (21). In fact, in the present study, intratracheal administration of BLM induced fibrotic changes in the lung, as indicated by histological findings (Ashcroft score) and lung hydroxyproline content. These findings were consistent with the results from earlier studies (17, 27). Because acute lung injury induced by a high dose of BLM (0.04 U/mouse) was too severe for mice to survive, a low dose of BLM (0.02 U/mouse) was used to evaluate the antifibrotic effect of CNP. Interestingly, 14-day infusion of CNP significantly decreased Ashcroft score and lung hydroxyproline content. Thus, in the present study, we first demonstrated that CNP infusion attenuated BLM-induced pulmonary fibrosis. However, the underlying mechanisms still remain unclear. Earlier studies have shown that pulmonary inflammation and fibroblast proliferation are responsible for pulmonary fibrosis in BLM-treated animals and humans (6, 21). Thus we inves-

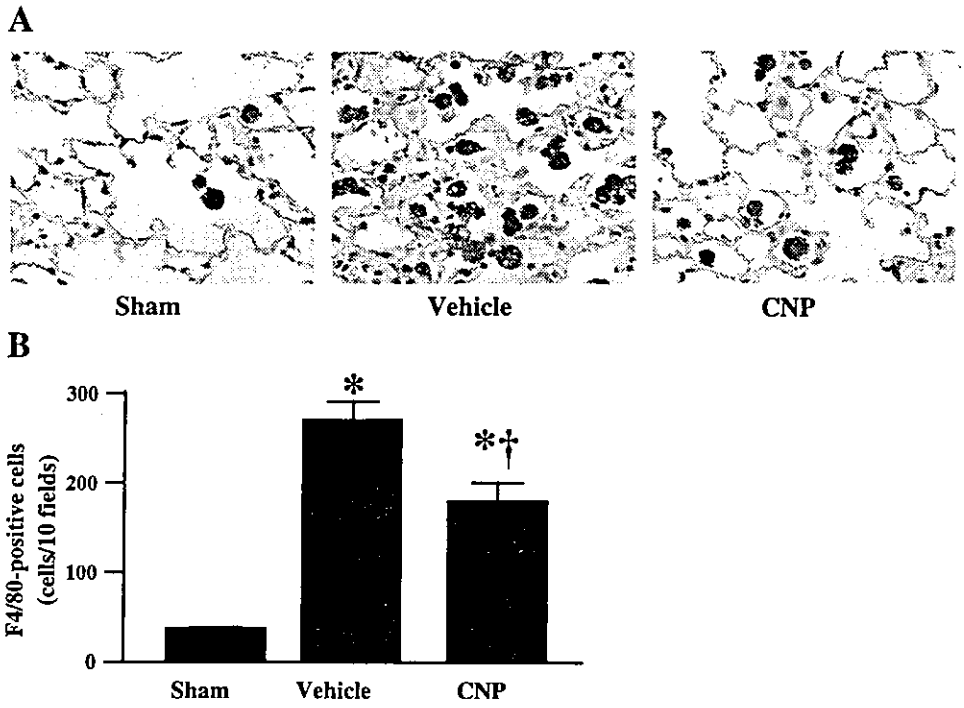

Fig. 5. *A*: immunohistochemical analysis of F4/80 antigen, a marker for monocytes/macrophages, 14 days after BLM injection. Histological sections were taken from the same general regions of the lungs in each group. Monocytes/macrophages were frequently observed in BLM mice given vehicle (vehicle group). CNP infusion markedly inhibited macrophage infiltration (CNP group). Magnification, ×400. *B*: semi-quantitative analyses of F4/80-positive cells in the lung. The number of F4/80-positive cells in the CNP group was significantly lower than that in the vehicle group. Data are means ± SE. *$P < 0.05$ vs. Sham group; †$P < 0.05$ vs. vehicle group.

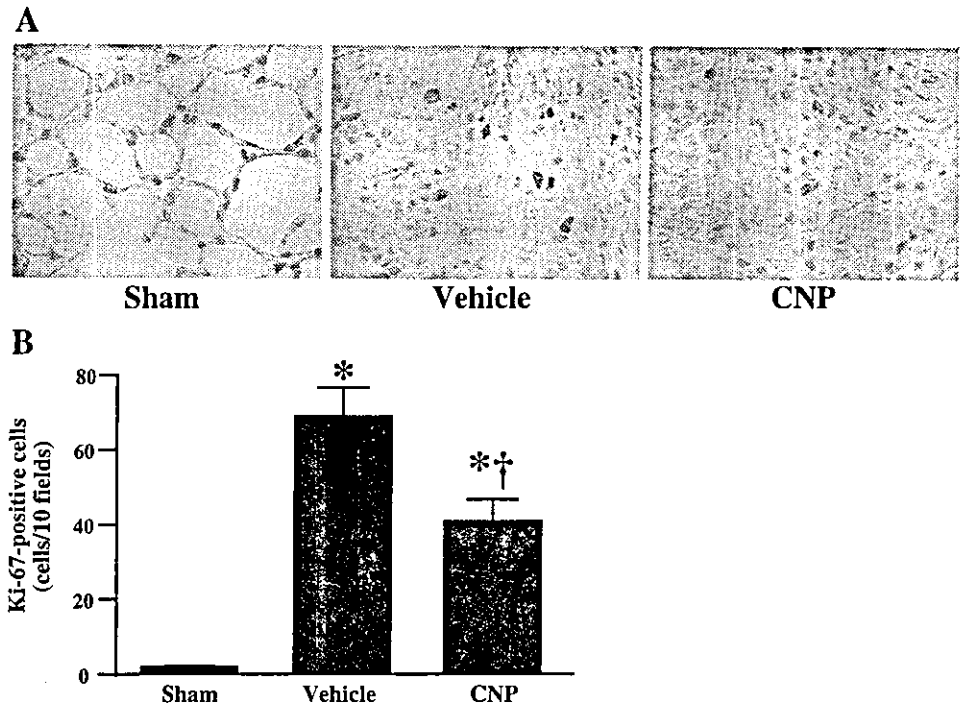

Fig. 6. *A*: immunohistochemical analysis of Ki-67 antigen, a marker for cell proliferation. Histological sections were taken from the same general regions of the lungs in each group. Ki-67-positive nuclei were detected mainly in fibrotic lesions 14 days after BLM injection (vehicle group). CNP infusion decreased the number of Ki-67-positive cells. Magnification, ×400. *B*: semi-quantitative analysis also demonstrated that the number of Ki-67-positive cells in the fibrotic lesions was significantly decreased in the CNP group. Data are means ± SE. $*P < 0.05$ vs. Sham group; $\dagger P < 0.05$ vs. vehicle group.

tigated whether CNP infusion inhibits pulmonary inflammation and fibroblast proliferation in vivo.

Several proinflammatory cytokines including IL-1β and TNF-α are involved in pulmonary inflammation and the subsequent development of pulmonary fibrosis in a mouse model of BLM-induced pulmonary fibrosis (3, 11, 18). A previous study showed that continuous infusion of an IL-1 receptor antagonist prevented BLM-induced pulmonary fibrosis (19). Moreover, BLM-stimulated alveolar macrophages released IL-1β, which can serve as a fibroblast growth factor (25). These findings implicate IL-1β as a key mediator in BLM-induced pulmonary fibrosis. In the present study, CNP infusion markedly inhibited the increase in BALF IL-1β levels after BLM injection, together with a significant decrease in the number of inflammatory cells in BALF. Immunohistochemical examination also demonstrated that CNP infusion significantly inhibited infiltration of macrophages into the alveolar and interstitial regions. A recent study has shown that CNP suppresses the expression of monocyte chemoattractant protein-1, which induces migration and activation of macrophages (16). Considering that IL-1β is mainly produced by activated alveolar macrophages, it is interesting to speculate that CNP inhibits IL-1β production via inactivation of macrophages. Neutrophils have been shown to induce lung parenchymal injury by producing toxic radical oxygen species and a variety of proteolytic enzymes in BLM-induced fibrosis (12, 13, 26). The recruitment of lymphocytes has been shown to precede the development of pulmonary fibrosis (10). In the present study, CNP significantly attenuated the increase in the numbers of neutrophils and lymphocytes in BALF. Thus CNP infusion may attenuate BLM-induced pulmonary fibrosis in part through inhibition of pulmonary inflammation.

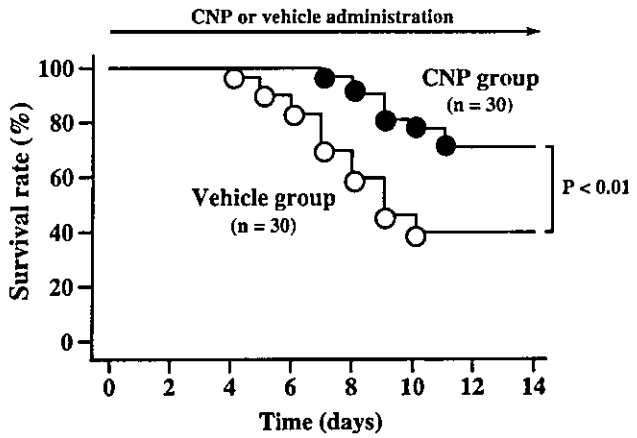

Fig. 7. Kaplan-Meier survival curves. BLM mice treated with CNP (●) had a significantly higher survival rate than those given vehicle (○) (log-rank test, $P < 0.01$).

Fibroblasts in fibrotic lesions have been considered to be the cells responsible for deposition of matrix (9). In addition, fibroblasts have been found to be significant sources of several cytokines, including transforming growth factor-β, a well-established key fibrogenic mediator, and monocyte chemoattractant protein-1 (28, 29). Thus pulmonary fibroblasts play an important role in the development of fibrosis in the lung. The present study demonstrated that BLM injection enhanced cell proliferation in the lung, as indicated by an increase in the number of Ki-67-positive cells in the fibrotic lesions. Interestingly, CNP infusion markedly inhibited Ki-67-positive cells in fibrotic lesions of the lung. An in vitro study showed that CNP directly inhibited proliferation of cardiac fibroblasts through a guanylate cyclase-B-mediated cGMP-dependent pathway (7). Thus it is possible that the reduction of pulmonary fibrosis by CNP infusion may be mediated by a direct antiproliferative effect of CNP on fibroblasts in the lung.

In the present study, continuous infusion of CNP significantly improved survival in BLM mice. Infusion of CNP

inhibited the development of pulmonary fibrosis and inflammation. As a result, CNP may have beneficial effects on survival in BLM mice. Considering that most patients with pulmonary fibrosis are refractory to conventional therapy, this therapy may be an alternative approach for severe pulmonary fibrosis. However, the initial success of CNP administration reported here should be confirmed by long-term experiments, and extensive toxicity studies in animals are needed before clinical trials.

In conclusion, continuous infusion of CNP attenuated BLM-induced pulmonary fibrosis and improved survival in BLM mice. These beneficial effects of CNP may be mediated at least in part by inhibition of pulmonary inflammation and cell proliferation. Thus CNP supplementation may be a new therapeutic strategy for the treatment of pulmonary fibrosis.

GRANTS

This work was supported by Research Grant for Cardiovascular Disease 16C-6 from the Ministry of Health, Labour, and Welfare; Industrial Technology Research Grant Program in '03 from New Energy and Industrial Technology Development Organization of Japan; Health and Labor Sciences Research Grants-genome 005; and the Promotion of Fundamental Studies in Health Science of the Organization for Pharmaceutical Safety and Research of Japan.

REFERENCES

1. **Ashcroft T, Simpson JM, and Timbrell V.** Simple method of estimating severity of pulmonary fibrosis on a numerical scale. *J Clin Pathol* 41: 467–470, 1988.
2. **Crouch E.** Pathobiology of pulmonary fibrosis. *Am J Physiol Lung Cell Mol Physiol* 259: L159–L184, 1990.
3. **Elias JA, Freundlich B, Kern JA, and Rosenbloom J.** Cytokine networks in the regulation of inflammation and fibrosis in the lung. *Chest* 97: 1439–1445, 1990.
4. **Geary CA, Goy MF, and Boucher RC.** Synthesis and vectorial export of cGMP in airway epithelium: expression of soluble and CNP-specific guanylate cyclases. *Am J Physiol Lung Cell Mol Physiol* 265: L598–L605, 1993.
5. **Gross TJ and Hunninghake GW.** Idiopathic pulmonary fibrosis. *N Engl J Med* 345: 517–525, 2001.
6. **Hay J, Shahzeidi S, and Laurent G.** Mechanisms of bleomycin-induced lung damage. *Arch Toxicol* 65: 81–94, 1991.
7. **Horio T, Tokudome T, Maki T, Yoshihara F, Suga S, Nishikimi T, Kojima M, Kawano Y, and Kangawa K.** Gene expression, secretion, and autocrine action of C-type natriuretic peptide in cultured adult rat cardiac fibroblasts. *Endocrinology* 144: 2279–2284, 2003.
8. **Komatsu Y, Nakao K, Itoh H, Suga S, Ogawa Y, and Imura H.** Vascular natriuretic peptide. *Lancet* 340: 622, 1992.
9. **Kuhn C and McDonald JA.** The roles of the myofibroblast in idiopathic pulmonary fibrosis. Ultrastructural and immunohistochemical features of sites of active extracellular matrix synthesis. *Am J Pathol* 138: 1257–1265, 1991.
10. **Kumar RK.** Quantitative immunohistologic assessment of lymphocyte populations in the pulmonary inflammatory response to intratracheal silica. *Am J Pathol* 135: 605–614, 1989.
11. **Maeda A, Hiyama K, Yamakido H, Ishioka S, and Yamakido M.** Increased expression of platelet-derived growth factor A and insulin-like growth factor-I in BAL cells during the development of bleomycin-induced pulmonary fibrosis in mice. *Chest* 109: 780–786, 1996.
12. **Mitsuhashi H, Asano S, Nonaka T, Hamamura I, Masuda K, and Kiyoki M.** Administration of truncated secretory leukoprotease inhibitor ameliorates bleomycin-induced pulmonary fibrosis in hamsters. *Am J Respir Crit Care Med* 153: 1369–1374, 1996.
13. **Nagai A, Aoshiba K, Ishihara Y, Inano H, Sakamoto K, Yamaguchi E, Kagawa J, and Takizawa T.** Administration of α1-proteinase inhibitor ameliorates bleomycin-induced pulmonary fibrosis in hamsters. *Am Rev Respir Dis* 145: 651–656, 1992.
14. **Nakanishi K, Tajima F, Itoh H, Nakata Y, Hama N, Nakagawa O, Nakao K, Kawai T, Torikata C, Suga T, Takishima K, Aurues T, and Ikeda T.** Expression of C-type natriuretic peptide during development of rat lung. *Am J Physiol Lung Cell Mol Physiol* 277: L996–L1002, 1999.
15. **Nakazawa K, Tanaka H, and Arima M.** Rapid, simultaneous and sensitive determination of free hydroxyproline and proline in human serum by high-performance liquid chromatography. *J Chromatogr A* 233: 313–316, 1982.
16. **Osawa H, Yamabe H, and Kaizuka M.** C-type natriuretic peptide inhibits proliferation and monocyte chemoattractant protein-1 secretion in cultured human mesangial cells. *Nephron* 86: 467–472, 2000.
17. **Phan SH, Thrall RS, and Williams C.** Bleomycin-induced pulmonary fibrosis. Effects of steroid on lung collagen metabolism. *Am Rev Respir Dis* 124: 428–434, 1981.
18. **Piguet PF, Collart MA, Grau GE, Kapanci Y, and Vassalli P.** Tumor necrosis factor/cachectin plays a key role in bleomycin-induced pneumopathy and fibrosis. *J Exp Med* 170: 655–663, 1989.
19. **Piguet PF, Vesin C, Grau GE, and Thompson RC.** Interleukin 1 receptor antagonist (IL-1ra) prevents or cures pulmonary fibrosis elicited in mice by bleomycin or silica. *Cytokine* 5: 57–61, 1993.
20. **Qian JY, Haruno A, Asada Y, Nishida T, Saito Y, Matsuda T, and Ueno H.** Local expression of C-type natriuretic peptide suppresses inflammation, eliminates shear stress-induced thrombosis, and prevents neointima formation through enhanced nitric oxide production in rabbit injured carotid arteries. *Circ Res* 91: 1063–1069, 2002.
21. **Snider GL, Hayes JA, and Korthy AL.** Chronic interstitial pulmonary fibrosis produced in hamsters by endotracheal bleomycin: pathology and stereology. *Am Rev Respir Dis* 117: 1099–1108, 1978.
22. **Sudoh T, Minamino N, Kangawa K, and Matsuo H.** C-type natriuretic peptide (CNP): a new member of natriuretic peptide family identified in porcine brain. *Biochem Biophys Res Commun* 168: 863–870, 1990.
23. **Suga S, Nakao K, Hosoda K, Mukoyama M, Ogawa Y, Shirakami G, Arai H, Saito Y, Kambayashi Y, Inouye K, and Imura H.** Receptor selectivity of natriuretic peptide family, atrial natriuretic peptide, brain natriuretic peptide, and C-type natriuretic peptide. *Endocrinology* 130: 229–239, 1992.
24. **Suga S, Nakao K, Itoh H, Komatsu Y, Ogawa Y, Hama N, and Imura H.** Endothelial production of C-type natriuretic peptide and its marked augmentation by transforming growth factor-β. Possible existence of "vascular natriuretic peptide system." *J Clin Invest* 90: 1145–1149, 1992.
25. **Suwabe A, Takahashi K, Yasui S, Arai S, and Sendo F.** Bleomycin-stimulated hamster alveolar macrophages release interleukin-1. *Am J Pathol* 132: 512–520, 1988.
26. **Taooka Y, Maeda A, Hiyama K, Ishioka S, and Yamakido M.** Effects of neutrophil elastase inhibitor on bleomycin-induced pulmonary fibrosis in mice. *Am J Respir Crit Care Med* 156: 260–265, 1997.
27. **Yaekashiwa M, Nakayama S, Ohnuma K, Sakai T, Abe T, Satoh K, Matsumoto K, Nakamura T, Takahashi T, and Nukiwa T.** Simultaneous or delayed administration of hepatocyte growth factor equally represses the fibrotic changes in murine lung injury induced by bleomycin. A morphologic study. *Am J Respir Crit Care Med* 156: 1937–1944, 1997.
28. **Zhang K, Flanders KC, and Phan SH.** Cellular localization of transforming growth factor-β expression in bleomycin-induced pulmonary fibrosis. *Am J Pathol* 147: 352–361, 1995.
29. **Zhang K, Gharaee-Kermani M, Jones ML, Warren JS, and Phan SH.** Lung monocyte chemoattractant protein-1 gene expression in bleomycin-induced pulmonary fibrosis. *J Immunol* 153: 4733–4741, 1994.

C-type Natriuretic Peptide Ameliorates Monocrotaline-induced Pulmonary Hypertension in Rats

Takefumi Itoh, Noritoshi Nagaya, Shinsuke Murakami, Takafumi Fujii, Takashi Iwase, Hatsue Ishibashi-Ueda, Chikao Yutani, Masakazu Yamagishi, Hiroshi Kimura, and Kenji Kangawa

Department of Regenerative Medicine and Tissue Engineering, National Cardiovascular Center Research Institute, Osaka; Second Department of Internal Medicine, Nara Medical University, Nara; Department of Internal Medicine, National Cardiovascular Center; Department of Cardiac Physiology, National Cardiovascular Center Research Institute; Department of Pathology, National Cardiovascular Center; and Department of Biochemistry, National Cardiovascular Center Research Institute, Osaka, Japan

C-type natriuretic peptide (CNP) has been shown to act as a local regulator of vascular tone and remodeling. We investigated whether CNP ameliorates monocrotaline (MCT)-induced pulmonary hypertension in rats. Rats received a continuous infusion of CNP or placebo. Significant pulmonary hypertension developed 3 weeks after MCT. However, infusion of CNP significantly attenuated the development of pulmonary hypertension and vascular remodeling. Neither systemic arterial pressure nor heart rate was altered. Interestingly, CNP enhanced Ki-67 expression, a marker for cell proliferation, in pulmonary endothelial cells and augmented lung tissue content of endothelial nitric oxide synthase. CNP significantly suppressed apoptosis of pulmonary endothelial cells, decreased the number of monocytes/macrophages, and inhibited expression of plasminogen activator inhibitor type 1, a marker for fibrinolysis impairment, in the lung. In addition, CNP significantly increased the survival rate in MCT rats. Finally, infusion of CNP after the establishment of pulmonary hypertension also had beneficial effects on hemodynamics and survival. In conclusion, infusion of CNP ameliorated MCT-induced pulmonary hypertension and improved survival. These beneficial effects may be mediated by regeneration of pulmonary endothelium, inhibition of endothelial cell apoptosis, and prevention of monocyte/macrophage infiltration and fibrinolysis impairment.

Keywords: monocrotaline; natriuretic peptides; pulmonary hypertension; vasoprotection

Primary pulmonary hypertension is a rare but life-threatening disease characterized by progressive pulmonary hypertension that leads to right ventricular (RV) failure and death (1). The common pathologic findings in primary pulmonary hypertension are endothelial cell injury, plexiform lesion, medial hypertrophy, infiltration of inflammatory cells, and thrombosis in small pulmonary arteries (2, 3). Endothelial dysfunction decreases the production of vasodilators such as prostacyclin and nitric oxide, whereas it increases that of vasoconstrictors, including thromboxane and endothelin-1 (4, 5). Infiltration of inflammatory cells, which release many cytokines and growth factors, contributes to the development of pulmonary vascular remodeling (6–8). Thrombosis obstructs small pulmonary arteries, which exaggerates pulmonary hypertension (4). Thus, a therapeutic strategy against these abnormalities may be effective for the treatment of primary pulmonary hypertension.

C-type natriuretic peptide (CNP), the third member of the natriuretic peptide family consisting of 22 amino acids (9), is secreted by vascular endothelial cells (10). CNP binds to natriuretic peptide receptor B, which bears a guanylate cyclase, induces generation of cGMP (11), and acts as a local regulator of vascular tone and remodeling (12). Its vasodilatory effect is much less potent than those of atrial natriuretic peptide and brain natriuretic peptide (9, 13). Nevertheless, CNP inhibits the proliferation of vascular smooth muscle cells (14) and has antiinflammatory and antithrombotic effects in blood vessels (15). Moreover, CNP has been shown to induce endothelial regeneration in the injured vasculature (14, 16, 17). These findings raise the possibility that CNP may improve pulmonary hypertension through multiple vasoprotective effects.

Thus, the purpose of this study was to investigate whether continuous infusion of CNP ameliorates monocrotaline (MCT)-induced pulmonary hypertension in rats.

METHODS

Animals

All protocols were performed in accordance with the guidelines of the Animal Care Ethics Committee of the National Cardiovascular Center Research Institute. Male Wistar rats weighing 80 to 100 g were used in this study. Rats were randomly given a subcutaneous injection of either 60-mg/kg MCT or 0.9% saline and assigned to receive a continuous infusion of CNP or placebo. This protocol resulted in the creation of three groups: sham rats given placebo (sham group, n = 8), MCT rats given placebo (placebo group, n = 8), and MCT rats treated with CNP (CNP group, n = 8). Another 10 rats were used to evaluate the acute hemodynamic effect of CNP. An additional 24 rats were used to examine the effect of CNP on established pulmonary hypertension. Finally, 48 rats were used to investigate the effect of CNP on survival in MCT rats.

Experimental Protocol

After the rats were anesthetized by intraperitoneal injection of pentobarbital (30 mg/kg), they were given a subcutaneous injection of either MCT or saline. Then, a micro-osmotic pump (Alzet) was filled with either CNP to deliver a dose of 0.75 μg/hour or 5% glucose vehicle and implanted subcutaneously between the scapulae. Two weeks after implantation, the pump was exchanged under anesthesia. The animals were maintained on standard rat chow.

Hemodynamic studies were performed on Day 21. A polyethylene catheter was inserted into the right carotid artery to measure mean arterial pressure and heart rate. A polyethylene catheter was inserted into the RV to measure RV pressure. After completion of the previously mentioned measurements, the ventricles and lungs were excised, dissected

(Received in original form April 2, 2004; accepted in final form August 25, 2004)

Supported by grants from New Energy and Industrial Technology Development Organization, the Mochida Memorial Foundation for Medical and Pharmaceutical Research, and the Promotion of Fundamental Studies in Health Science of the Organization for Pharmaceutical Safety and Research of Japan.

Correspondence and requests for reprints should be addressed to Noritoshi Nagaya, M.D., Department of Regenerative Medicine and Tissue Engineering, National Cardiovascular Center Research Institute, 5-7-1 Fujishirodai, Suita, Osaka 565-8565, Japan. E-mail: nagayann@hsp.ncvc.go.jp

Am J Respir Crit Care Med Vol 170. pp 1204–1211, 2004
Originally Published In Press as DOI: 10.1164/rccm.200404-455OC on August 27, 2004
Internet address: www.atsjournals.org

free, and weighed. The ratio of RV weight to body weight, the ratio of RV weight to left ventricular plus septal weight, and the ratio of left ventricular plus septal weight to body weight were calculated as indexes of ventricular hypertrophy.

Morphometric Analysis of Pulmonary Arteries

We analyzed the medial wall thickness of the pulmonary arteries in the middle region of the right lung as described previously (18). The external diameter and the medial wall thickness were measured in 20 muscular arteries (ranging in external diameter from 25 to 100 μm) per rat. The medial wall thickness was expressed as follows: percentage of wall thickness = ([medial thickness × 2]/external diameter) × 100.

Immunohistochemical Analysis

Paraffin sections 4 μm thick were obtained from the right lung on Days 7 and 21 from individual rats for comparison among the three groups. To investigate whether CNP induces endothelial regeneration, tissue sections were stained for Ki-67, a marker for cell proliferation, using monoclonal anti-Ki-67 antibody (Dako, Copenhagen, Denmark). Paraffin sections were also stained with a rabbit polyclonal antibody raised against factor VIII (Dako), a mouse monoclonal antibody raised against rat monocyte/macrophage (ED1; Serotec, Oxford, UK), and a rabbit polyclonal antibody raised against plasminogen activator inhibitor type 1 (PAI-1) (Santa Cruz Biotechnology, Santa Cruz, CA). To detect apoptosis in pulmonary endothelial cells 1 week after MCT injection, terminal dUTP nick-end labeling assays were performed using a commercially available kit (ApopTag Plus; Intergen, New York, NY). The number of Ki-67–positive endothelial cells per mm^2 was determined under light microscopy. The numbers of alveoli and factor VIII-positive capillaries (< 100 μm in diameter) were counted. Capillary density was expressed as the number of capillaries per 100 alveoli. The number of ED1-positive cells was determined in 10 randomly chosen high-power fields (×400). The percentage of PAI-1–positive endothelial cells was calculated (number of PAI-1–positive endothelial cells/total number of endothelial cells × 100) in 10 randomly chosen high-power fields (×400). The number of terminal dUTP nick-end labeling–positive endothelial cells per section was calculated. Histologic analysis was performed in a blinded fashion by two observers.

Western Blot Analysis

To identify endothelial nitric oxide synthase, Western blotting was performed using a mouse monoclonal antibody raised against endothelial nitric oxide synthase (Transduction Laboratories, Lexington, KY) as previously described (19). Western blot analysis using a mouse polyclonal antibody against β-actin (Santa Cruz) was used as a protein loading control. Peripheral samples of lung tissue were obtained on Day 21 from individual rats for comparison among the three groups (sham, placebo, and CNP groups, n = 8 each). Endothelial nitric oxide synthase protein was shown as the percentage of the level expressed in sham rats.

Acute Hemodynamic Study

To investigate the acute hemodynamic effects of CNP and atrial natriuretic peptide, CNP (0.05 μg/kg/min) or atrial natriuretic peptide (0.05 μg/kg/min) was intravenously administered at 3 weeks after MCT injection (n = 5 each). Hemodynamics were measured at 15-minute intervals before, during, and after infusion, and the effect of CNP was compared with that of atrial natriuretic peptide.

Delayed Therapy

To investigate the effect of CNP on established pulmonary hypertension, 24 rats were randomly given an injection of either MCT or saline. Three weeks after MCT injection, the animals received continuous infusion of CNP or placebo for 1 week (sham, placebo, and CNP groups, n = 8 each). These rats were evaluated on Day 28.

Survival Analysis

To evaluate the effect of CNP on survival in MCT rats, 24 rats received continuous infusion of CNP (n = 12) or placebo (n = 12) immediately after MCT injection. Another 24 rats received continuous infusion of CNP (n = 12) or placebo (n = 12) 3 weeks after MCT injection. Survival was estimated from the date of MCT injection to the death of the rat or 8 weeks after MCT injection.

Statistical Analysis

All data were expressed as mean ± SEM unless otherwise indicated. Comparisons of parameters among the three groups were made by one-way analysis of variance, followed by Newman-Keul's test. Survival curves were derived by the Kaplan-Meier method and compared by log-rank test. A value of p less than 0.05 was considered statistically significant.

RESULTS

Physiologic and Morphologic Assessment

The physiologic profiles of the three experimental groups are summarized in Table 1. Body weight was significantly lower in MCT rats than in sham rats. The ratio of RV weight to body weight was significantly increased after MCT injection (Figure 1A). However, CNP infusion significantly attenuated the increase in the ratio of RV weight to body weight compared with placebo.

Hemodynamics

RV systolic pressure was significantly increased 3 weeks after MCT injection (Figure 1B). However, CNP infusion significantly attenuated the increase in RV systolic pressure compared with placebo. There was no significant difference in mean arterial pressure or heart rate among the three groups (Table 1).

Morphometric Analysis of Pulmonary Arteries

Representative photomicrographs showed that CNP infusion significantly inhibited hypertrophy of the pulmonary vessel wall compared with placebo (Figure 1C). Quantitative analysis of peripheral pulmonary arteries demonstrated a significant increase in percentage wall thickness after MCT injection, but the increase in the CNP group was significantly inhibited compared with that in the placebo group (Figure 1D).

Endothelial Regeneration

The number of Ki-67–positive endothelial cells was significantly increased in the CNP group compared with the placebo group (Figures 2A–2D). The number of terminal dUTP nick-end labeling–positive pulmonary endothelial cells was significantly increased 1 week after MCT injection (Figure 2E). CNP infusion significantly decreased the number of terminal dUTP nick-end labeling–positive pulmonary endothelial cells. Although the capillary density was significantly decreased after MCT injection, CNP significantly increased the capillary density (Figures 3A–3D). Western blot analysis showed that lung tissue content of endothelial nitric oxide synthase protein was significantly decreased after MCT injection (Figures 3E and 3F). However, CNP infusion increased lung tissue content of endothelial nitric oxide synthase protein in MCT rats.

Monocyte/Macrophage Infiltration

Representative photomicrographs showed that CNP infusion markedly inhibited monocyte/macrophage infiltration into the alveolar spaces compared with placebo (Figures 4A–4C). Quantitative analysis demonstrated a significant increase in the number of monocytes/macrophages after MCT injection, but the increase in the CNP group was markedly inhibited compared with that in the placebo group (Figure 4D).

PAI-1 Expression

Representative photomicrographs demonstrated that CNP infusion markedly inhibited PAI-1 expression in pulmonary endothelial cells

TABLE 1. PHYSIOLOGIC PROFILES OF EXPERIMENTAL GROUPS

	Sham	Placebo	CNP
n	8	8	8
BW, g	195 ± 4	173 ± 8*	179 ± 3*
Heart rate, bpm	431 ± 14	455 ± 15	447 ± 13
MAP, mm Hg	124 ± 3	122 ± 4	123 ± 4
RV systolic pressure, mm Hg	35 ± 3	66 ± 4*	51 ± 3*†
RV/BW, g/kg body weight	0.55 ± 0.01	0.95 ± 0.03*	0.74 ± 0.03*†
RV/LV + S, g/g	0.25 ± 0.02	0.40 ± 0.02*	0.31 ± 0.01*†
LV + S/BW, g/kg body weight	2.21 ± 0.04	2.42 ± 0.05	2.36 ± 0.04

Definition of abbreviations: bpm = beats per minute; BW = body weight; CNP = C-type natriuretic peptide; LV + S/BW = ratio of left ventricular plus septal weight to body weight; MAP = mean arterial pressure; RV = right ventricular; RV/BW = ratio of RV weight to body weight; RV/LV + S = ratio of RV weight to left ventricular plus septal weight.

*$p < 0.05$ vs. sham.

†$p < 0.05$ vs. placebo.

These measurements were performed on Day 21. Data are mean ± SEM.

compared with placebo (Figures 5A–5C). Semiquantitative analysis demonstrated a significant increase in the number of plasminogen activator inhibitor type 1 (PAI-1)–positive endothelial cells after MCT injection (Figure 5D). However, the increase in PAI-1–positive cells was significantly inhibited by CNP infusion.

Acute Hemodynamic Effect

Infusion of atrial natriuretic peptide significantly decreased RV systolic pressure and mean arterial pressure (Figure 6). In contrast, CNP did not significantly alter any hemodynamic parameters.

Delayed Therapy

Delayed CNP therapy slightly but significantly attenuated the increases in the ratio of RV weight to body weight and RV systolic pressure compared with placebo (Figures 7A and 7B). There was no significant difference in mean arterial pressure or heart rate among the three groups (data not shown). Morphometric analysis of pulmonary arteries demonstrated that delayed CNP therapy significantly attenuated hypertrophy of the medial wall (Figures 7C and 7D).

Survival Analysis

Kaplan-Meier survival curves demonstrated that rats treated with CNP immediately after MCT injection had a markedly higher survival rate than those given placebo (50% vs. 0% in 8-week survival, log-rank test, $p < 0.001$; Figure 8A). In addition, delayed CNP therapy also increased the survival rate in MCT rats compared with placebo (25% vs. 0% in 8-week survival, $p < 0.01$; Figure 8B).

DISCUSSION

In this study, we demonstrated that (*1*) continuous infusion of CNP ameliorated MCT-induced pulmonary hypertension and vascular remodeling and that (*2*) CNP infusion improved survival in MCT rats without definite adverse effects. We also dem-

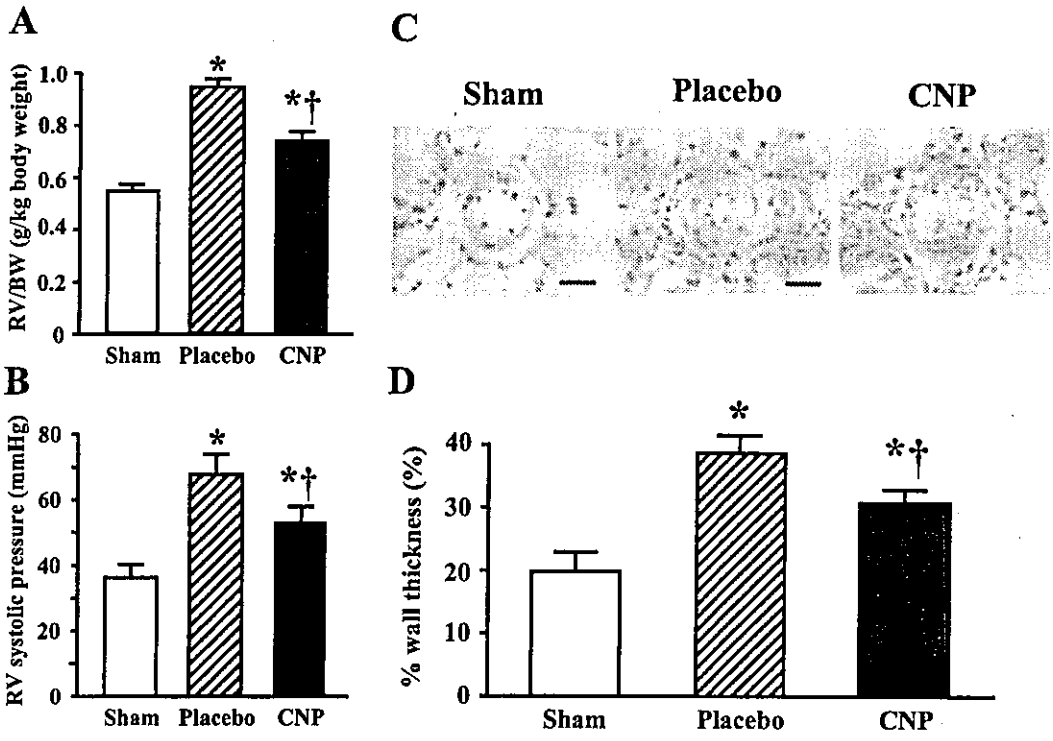

Figure 1. Effects of C-type natriuretic peptide (CNP) infusion on developing pulmonary hypertension. Continuous infusion of CNP was initiated immediately after monocrotaline (MCT) injection. (*A*) Right ventricular (RV) weight to body weight (RV/BW). (*B*) RV systolic pressure. (*C*) Representative photomicrographs of peripheral pulmonary arteries. *Scale bars* = 20 μm. (*D*) Quantitative analysis of percentage wall thickness in peripheral pulmonary arteries. Data are mean ± SEM. *$p < 0.05$ versus sham; †$p < 0.05$ versus placebo.